TRANS NOW
TRANSPORTATION NORTHWEST

Final Report TNW2012-08

Research Project Agreement No. 62-0985

Evaluation of Gusset Plate Safety in Steel Truss Bridges

Jeffrey W. Berman, Assistant Professor
Civil and Environmental Engineering
University of Washington

A report prepared for

Transportation Northwest (TransNow)
University of Washington
112 More Hall, Box 352700
Seattle, Washington 98195-2700

November 2011

TECHNICAL REPORT STANDARD TITLE PAGE

1. REPORT NO. TNW2012-08	2. GOVERNMENT ACCESSION NO.	3. RECIPIENT'S CATALOG NO.	
4. TITLE AND SUBTITLE Evaluation of Gusset Plate Safety in Steel Truss Bridges		5.REPORT DATE 11/2011 6. PERFORMING ORGANIZATION CODE 62-0985	
7. AUTHOR(S) Jeffrey Berman		8. PERFORMING ORGANIZATION REPORT NO. TNW2012-08	
9. PERFORMING ORGANIZATION NAME AND ADDRESS Transportation Northwest Regional Center X (TransNow) Box 352700, 112 More Hall University of Washington Seattle, WA 98195-2700		10. WORK UNIT NO. 11. CONTRACT OR GRANT NO. DTRT07-G-0010	
12. SPONSORING AGENCY NAME AND ADDRESS United States Department of Transportation Office of the Secretary of Transportation 1200 New Jersey Ave, SE Washington, D.C. 20590		13. TYPE OF REPORT AND PERIOD COVERED Final Technical Report 14. SPONSORING AGENCY CODE	
15. SUPPLEMENTARY NOTES			
ABSTRACT Failure of the I-35 truss bridge in Minneapolis has been attributed to failure of a gusset plate, necessitating evaluation of gusset plate safety on bridges across the county. FHWA Publication IF-09-014 provides state DOTs with important guidance for gusset plate evaluation but the methods are unnecessarily complex, requiring the use of point-in-time demands which are cumbersome to calculate, and do not investigate the likelihood of plate yielding under service loads, which may compromise plate safety. With support from WSDOT and FHWA, the PI's are developing a simpler and consistent evaluation method using finite element analyses (FEAs). The resulting Triage Evaluation Procedure (TEP) improves the speed, consistency and safety of gusset plate evaluation by predicting the onset gusset plate yielding, which permits evaluation of the likelihood of inelastic response under service conditions using envelope loads, thereby decreasing computation time while maintaining an appropriate level of conservatism. The TEP will save time and money relative to the FHWA method, while predicting safety. This proposal addresses research needed to evaluate gussets identified as potentially unsafe by the TEP, the likelihood of rivet yielding or failure, and the impact of corrosion. First, a practical, but more refined evaluation procedure (REP) will be furthered to evaluate gusset plates that fail the TEP in lieu of impractical detailed finite element modeling. The REP will be grounded in mechanics and verified by comparison with detailed FEA results for many gusset plate configurations. Second, the strength of older rivets will be investigated by reviewing experimental results from the literature; the rivet strengths specified in the FHWA Guide are conservative, which may result in unnecessary and costly rivet replacement. Third, the correct application of TEP and REP to corroded gusset plates, a common problem with national impact, will be investigated.			
17. KEY WORDS Bridge, gusset plates		18. DISTRIBUTION STATEMENT No restrictions.	
19. SECURITY CLASSIF. (of this report) None	20. SECURITY CLASSIF. (of this page) None	21. NO. OF PAGES 84	22. PRICE

DISCLAIMER

The contents of this report reflect the views of the authors, who are responsible for the facts and the accuracy of the information presented herein. This document is disseminated under the sponsorship of the Department of Transportation University Transportation Centers Program, in the interest of information exchange. The U.S. Government assumes no liability for the contents or use thereof.

Table of Contents

List of Figures

List of Tables

Section 1 Introduction

1.1 Problem Statement

A Federal Highway Administration (FHWA) report (Ocel and Wright 2008) has demonstrated that several of the gusset plates in the I-35 Mississippi River Bridge in Minneapolis were significantly overstressed and has identified the inelastic buckling of one of the gusset plates as a likely initiator of the bridge collapse. Thus, there is an urgent need to evaluate the safety of gusset plates on such bridges across the county. In response, FHWA has released *Load Rating Guidance and Examples for Bolted and Riveted Gusset Plates in Truss Bridges* (FHWA Guide, FHWA 2009), which provides Departments of Transportation (DOTs) with guidance for gusset plate evaluation. In addition to checking the resistance of fasteners, the recommended approach includes four plate checks: compressive buckling, tension, shear and block shear. The shear check requires point-in-time truss element loads (denoted as concurrent loads) for consistent estimation of the shear stress, rather than envelope loads. This requirement can make the check cumbersome and time consuming. While it is important that gusset plates be evaluated for safety, the number of truss bridges that have failed relative to the total number of truss bridges in service suggests that the number of overstressed gusset plates on steel truss bridges throughout the U.S. is small. Thus, a rapid evaluation procedure that is appropriately conservative but can be easily and cost-effectively applied is needed. The procedure should identify gusset plates that may be overstressed and that warrant more detailed investigation, while permitting identification of the many others that clearly do not have a safety concern.

1.2 Objectives

The primary objective of this study is to develop a procedure for the safe, consistent and rapid evaluation of gusset plate connections in steel truss bridges. The method will be broadly applicable and utilize member envelope loads rather than concurrent loads to minimize the number of load cases that must be considered for each joint. The procedure will also be demonstrated to be conservative relative to those in the FHWA Guide such that it may be employed in lieu of those methods.

1.3 Scope of Work

To achieve the objective above the following tasks have been executed:

1. Review of FHWA methods for evaluating steel truss bridge gusset plate connections and other pertinent previous research and on-going studies.
2. Select joints from WSDOT bridges, in collaboration with WSDOT engineers, to study in detail for the development of the rapid joint evaluation procedure.
3. Develop detailed finite element models of the selected joints to study the general joint behavior including the onset of gusset plate yielding and buckling. Consider the effects of parameters such as joint geometry, gusset plate thickness and distribution of connecting member loads explicitly in a parametric study using the developed finite element models.
4. Develop a rapid evaluation procedure, denoted the triage evaluation procedure (TEP) based on simple mechanics and observations from the simulations. Both checks for gusset plate yielding and gusset plate buckling are included.
5. Use the finite element models to compare the ability of the TEP and the methods in the FHWA Guide to predict the onset of gusset plate yielding and buckling.
6. Apply the TEP to load rate three WSDOT bridges to ensure it is conservative relative to the FHWA Guide procedures and to ensure it is not overly conservative.
7. Load rate the same bridges considering the rivet strength limit state to investigate the conservativeness of the rivet strengths given in the FHWA Guide.
8. Review rivet test data from the literature on rivet yield and ultimate strengths and compare them with the FHWA Guide recommendations.
9. Develop a spreadsheet for implementation of the TEP and provide it to the WSDOT Bridge Preservation Office.
10. Formulate conclusions and recommendations for future research.

Section 2 Review of Previous Research and Recommendations

2.1 Previous Gusset Plate Research

The strength and behavior gusset plate connections in both steel truss bridges and braced frames in steel buildings have been studied, with the latter being the focus of the majority studies. Bridge gusset plates differ from those in buildings because: (i) they typically have multiple diagonal members connected, (ii) they often serve as chord splices, (iii) are subjected to fatigue (iv) are used in gusset pairs rather than single plates, and (v) are expected remain essentially elastic (in a building, braced frame gusset plates designed for seismic loading are expected to withstand significant inelastic deformation). Whitmore (1952) proposed that the maximum uniaxial stress in a gusset plate at the end of a connected axially loaded member can be approximated by assuming a uniform distribution over a defined width, known as the Whitmore effective width. A 30° dispersion angle is assumed to calculate the Whitmore effective width as shown in Figure 2-1a. The connection length in the longitudinal direction of the member is taken as the distance from the first connector (e.g. bolt, rivet, or initiation of weld) to the end of the connection or last connector. The predicted maximum uniaxial stress is the member axial load divided by the Whitmore width times the gusset plate thickness. In his experiments, Whitmore demonstrated that this assumption provided a conservative estimate of the maximum uniaxial gusset plate stresses at the ends of members. Bjorhovde and Chakrabarti (1985) demonstrated that the Whitmore width concept was valid for gusset plates in braced frames and also demonstrated the method was appropriate for predicting net section fracture. Hardash and Bjorhovde (1985) studied braced frame gusset plate connections in tension and developed a block shear model based on a combination of shear and tension net section fracture. Other recent studies such as Yam and Chang (2002), Sheng et al (2002), and Yoo et al. (2008) have investigated the seismic performance of gusset plate connections in braced frames under inelastic tension, compression, and/or cyclic loading.

Several models for estimating the buckling strength of gusset plates have been proposed. Thornton (1984) suggested the use of the Whitmore width and an unbraced gusset plate length that is the average of the three lengths, as shown in Figure 2-1b, for use in standard buckling equations. Yam (1994) developed the Modified Thornton Method for estimating the buckling capacity, which accounts for load redistribution caused by yielding in the gusset plates prior to stability failure. The Modified Thornton Method uses a stress dispersion angle of 45° and an unbraced length in the longitudinal direction of the brace that extends from the centroid of the brace at the last row of fasteners to the first intersection with gusset plate support as shown in

Figure 2-1c. Brown (1988) and Astaneh-Asl (1989) both proposed gusset plate buckling models that are functions of the unsupported free edge length, again based on testing of typical gusset plate configurations for braced frames in buildings. Roeder et al. (2005) and Yoo (2006) collected gusset plate buckling data from the literature and used it to compare the various methods of predicting gusset buckling. A hybrid of the Thornton and Modified Thornton Methods that uses a 45° dispersion angle and the average of the three unsupported lengths, as shown in Figure 2-1d, was recommended (denoted as the Yoo method herein).

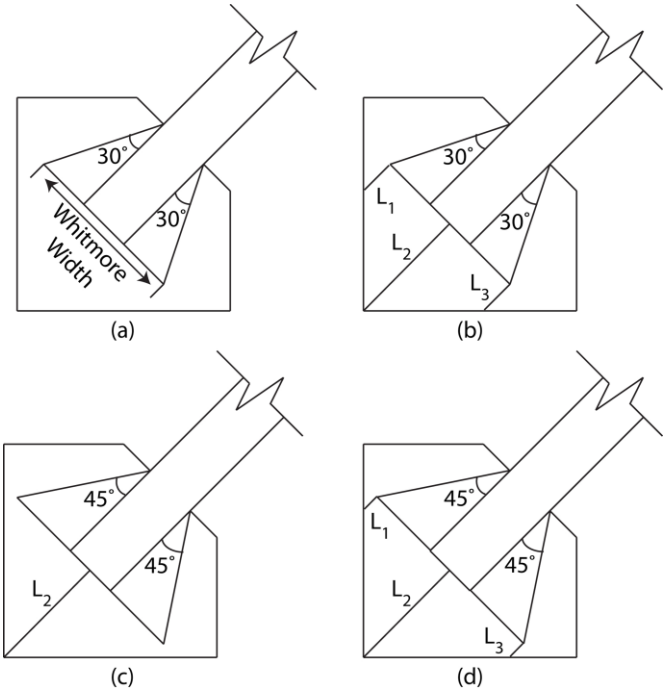

Figure 2-1 (a) The Whitmore Effective Width Concept, (b) Thornton Method for Unbraced Length, (c) Modified Thornton Method for Unbraced Length, (d) Yoo Method for Unbraced Length

Following the collapse of the I-35 Bridge in Minneapolis there has been a renewed interest in the behavior of steel truss bridge gusset plates. Ocel and Wright (2008) performed a detailed analysis of the I-35 Bridge. They developed several global models of the bridge and approach spans representing the assumed state of the bridge when it opened in 1965 and also as it existed in 2007. In one set of models of the 2007 state of the bridge, four highly stressed joints were modeled with detailed shell element models, these were Joints U10 and L11 on both the east and west trusses. The deck was modeled with shell elements and was connected to the truss structure with spring elements. The piers were modeled and pinned boundary conditions were used at the foundation except as explained below and the connections with the truss were assumed to be ideal (i.e., pins and rollers) except as explained below. The bridge was analyzed in four steps as follows:

- Step 1 simulated construction loading with the deck elements deactivated and the weight of wet concrete added. Only dead loads were applied and point loads at the end of the truss were used to simulate the loads from the approach spans.
- Step 2 simulated the bridge just after construction where the weight of the wet concrete was removed and the deck elements were reactivated (with the deck's self-weight included in the elements). Additional loading was added to simulate the weight of concrete barriers.
- Step 3 simulated the bridge after modifications were made to the concrete barriers and additional weight was added to the deck to account for the additional deck thickness added over the years.
- Step 4 simulated the loads believed to be on the bridge at the time of collapse based on NTSB 07-115 (NTSB 2008). The bridge's boundary conditions were also modified at this stage. The bearings were fixed to the piers to simulate conditions observed during previous live load monitoring of the bridge.

The analyses of the bridge and gusset plate connections indicated that the gusset had significant yielding under the Step 2 dead loads. The yielding increased as additional load was added to the bridge and by Step 4 a large percentage of the gusset plate at Joint U10 was yielded. Failure of the bridge was simulated when the increased stress and deformation due to initial imperfections for Joint U10 were added. Photos of Joint U10 from prior to the collapse indicated that a vertical free edge of the gusset was bulged to a magnitude of between 12.7 mm (0.5 in.) to 25.4 mm (1 in.). With an in initial imperfection of 19.1 mm (0.75 in.) the gusset plate at U10 buckled under the compression diagonal and the bridge suffered a global instability.

Several other issues were investigated such as thermal movements of the bridge, corrosion at Joint L11, and the effect of deck stiffness. Simulation of the corrosion at Joint 11 was done by modifying the thickness of elements in the area where corrosion was noted. However, the simulation did not change the predicted failure mode of the bridge. Neither thermal movements nor changes in deck stiffness for cracking were found to significantly impact the stress distribution in the gusset plates. Based on these simulations, the Ocel and Wright (2008) concluded that buckling of the gusset plate of Joint U10 was a likely cause of the collapse. Notably, all observed buckling occurred after significant yielding of the gusset.

Higgins et al. (2010) compared block shear and Whitmore section methods for load rating existing steel truss bridges. The research highlights the fact that vintage steel bridge gusset plates

were designed using allowable stress design and Whitmore section approaches but will be load rated using load and resistance factored rating at strength levels using both Whitmore section approaches and block shear. Differences in the outcomes of rating the gussets at the allowable stress and maximum strength levels are identified and simplifications for rating are proposed. A set of equations for expected LRFR ratings were developed using random sampling and statistical analysis of several bridges. A method for determining a gusset plate connection design error was proposed by comparing the actual rating factor to the expected rating factor from the statistically based equations. The researchers concluded that many bridges designed using Whitmore section methods will produce rating factors less than 1.0. Two example applications of the proposed procedure were provided. Notably, other limit states recommended for load rating by FHWA as described below were not included in the proposed rating factor equations.

2.2 FHWA Load Rating Guidance

The resistance equations in the FHWA Guide are intended to provide for collapse prevention and are required to be checked for only strength load combinations for Load and Resistance Factor Rating (LRFR) or for maximum loads in Load Factor Rating (LFR). The FHWA Guide states that owners may require that connections be evaluated at other loads levels to minimize serviceability concerns.

Gusset plate strength in tension is governed by the limit states of gross section yield, net section fracture and block shear. The gross or net areas for gusset plates in tension are calculated using the Whitmore method (Figure 2-1a), which assumes a 30° dispersion angle for tension stresses as they are delivered from the tension member to the gusset plate. The block shear strength of the member connections to the gusset plate is evaluated using a standard block shear check that considers combined tension yielding and shear fracture or tension fracture and yielding.

Gusset plate shear strength is evaluated by considering uniform shear stress distributions across several possible sections as illustrated in Figure 2-2. For LFR, checks of both shear yield on the gross sections (Lines A-A and C-C in Fig. 2) and shear fracture on net sections (Lines B-B and D-D) are required using:

$$R_r = 0.58F_y A_g \Omega \qquad \textit{and} \qquad R_r = 0.85\left(0.58F_y A_n\right) \tag{2-1}$$

where A_g is gross area along a shear section, A_n is the net area along a shear section, and Ω is a reduction factor for the potential of shear buckling along a section. For gusset plates with ample

stiffness to prevent buckling and develop the full plastic shear force Ω is 1.00 and is 0.74 where this cannot be demonstrated. For the LRFR method a resistance factor, φ_{vy}, of 0.95 for yielding on the net section is applied and a resistance factor, φ_{vu}, of 0.80 is applied for net section shear, the latter replacing the 0.85 in Eq. 2-1.

The compressive strength of gusset plates is calculated per AASHTO LRFD Articles 6.9.2.1 and 6.9.4 (AASHTO 2007), which are essentially the column compression strength equations from the 2002 AISC Specifications for Steel Buildings (AISC 2002). The unbraced length for gusset plate compression as specified in the FHWA Guide is found from the Thornton method as shown in Figure 2-1b. The effective length coefficient, *K*, is determined from the six basic sway and non-sway cases commonly considered in compression member design and ranges from 0.65 to 2.1.

For design of new gusset plates a maximum slenderness ratio for unsupported edges of gusset plates is given as $2.06\sqrt{E/F_y}$, where *E* is the modulus of elasticity. For existing gussets this limit is not required to be satisfied, however, owners are advised to evaluate the cause and effect of out of flatness at unsupported edges of gusset plates. An earlier draft of the FHWA Guide also included a strength calculation for combined flexural and axial loads derived from flexural theory that has since been removed with the explanation that gusset plates are deep members and flexural theory is not applicable.

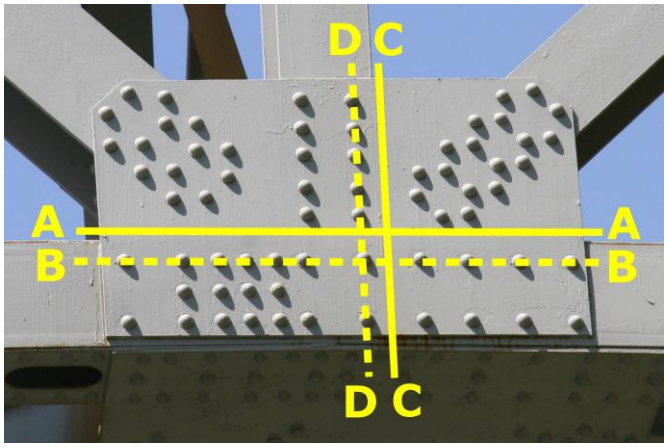

Figure 2-2 Typical Sections for Evaluating Shear Strength

Section 3 Global Bridge Analyses and Joint Selection

3.1 General

Three WSDOT bridges were selected for use in this study. Global analysis of the three bridges was performed to identify joints with relatively high stresses and unique geometry for use in the detailed finite element analyses described later. This section describes the three selected bridges, the global bridge analyses performed, validation of the models used, and the selection of specific joints for detailed finite element analysis.

3.2 Global Bridge Modeling Approach

Each bridge was modeled for global response using a linear-elastic analysis facilitated by SAP2000 (CSI 2008). In the interest of simplicity it was determined that the bridges could be effectively modeled as a two dimensional, plane truss. This greatly expedited the development of the models and still provides an adequate representation of the actual bridge loads. Truss members were modeled as having only axial forces, i.e., they did not transfer shear and moment at their ends. For comparison, the bridges were also modeled as frames without the moment releases and the differences in axial loads and the magnitudes of the induced moments proved to be negligible.

Some of the truss members on the bridges were constructed using built-up sections fastened together with rivets. It was assumed that the individual elements of the built-up member are attached to one another sufficiently enough to act as a single section. For built-up box sections, hand holes were spaced at regular intervals to provide access for maintenance. The cross-sectional area of these sections was reduced based on the number of hand holes along its length. This was done by calculating weighted area over the member length.

3.3 Selected WSDOT Bridges

3.3.1 Bridge BR 90-134N

Bridge BR 90-134N is a 220 ft. long, single span through truss bridge that carries two lanes of traffic in one direction; a photo of which can be seen in Figure 3-1. The shop drawings for BR 90-134N are dated 1949 and ASTM A7 steel was specified for the members and ASTM A94-46 steel (ASTM 1946) was specified for the gusset plates and splice plates. Figure 3-2 shows the naming convention used for each of the nodes on the bridge. At the support node L0, the design drawings show a pinned support and at support node L8 there is a roller support. The pin support allows

for free rotation of the node, but restrains the horizontal and vertical movement. The roller support allows for free rotation, vertical and horizontal motion.

Figure 3-1 Photo of BR 90-134N

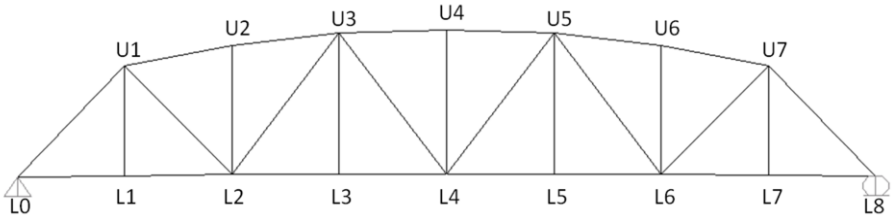

Figure 3-2 Schematic of BR 09-134N

Along the lower chords of the two identical trusses span floor beams which support the bridge deck and vehicular traffic. These floor beams frame directly into the joints of the main bridge trusses and so dead and live loads from the bridge deck are modeled as point loads at the bridge panel points. Along the top chord of the truss, wind bracing frames into the panel points and dead loads associated with these members are modeled as point loads at the nodes.

3.3.2 Bridge BR 31-36

Bridge BR 31-36 is a deck truss bridge that has two cantilever spans supporting a simple drop-in span in the middle. The bridge is 524 ft. long and has two main support piers approximately 142 ft. measured from each end of the bridge, as seen in Figure 3-3. The shop drawings for BR 31-36 are dated 1950 and all steel was specified as ASTM A7 which was taken to be ASTM A7-39 (ASTM 1939) with a specified yield stress of 228 MPa (33 ksi) (Brockenbrough 2002). Figure

3-4 shows the naming convention for the nodes; however, in the interest of space only half of the bridge is shown.

Figure 3-3 Photo of BR 31-36

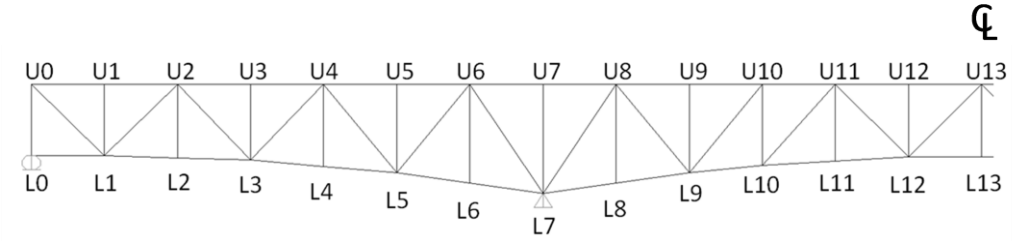

Figure 3-4 Schematic of BR 31-36

The design drawings indicate a pin support at node L7 and a roller support at node L0. Boundary conditions for this bridge were symmetric, so similar support conditions were assigned to the corresponding nodes on the remaining half of the bridge. Sliding pin assemblies are present between nodes U10-U11 and nodes L9-L10 to allow for thermal movement of the drop in simple span. These pin assemblies ensure no axial force is transmitted along these members, effectively making them zero-force members. To model these sliding pin assemblies, axial force releases were assigned at the ends of the frame members where each assembly is located.

The roadway is carried by floor beams that span across the two top chords of the identical main bridge trusses. These floor beams rest directly on top of the chord at each panel point and so dead and live loads attributed to the road deck are modeled as point loads at the nodes. Dead loads

associated with wind bracing and other structural elements that act along the bottom chord are also modeled as point loads at their corresponding nodes.

3.3.3 Bridge BR 101-217

Bridge BR 101-27 is also a deck truss bridge that has two cantilever spans that support a simple drop-in span in the middle. It is 392 ft. long with two main support piers approximately 71 ft. measured from each end of the bridge. The shop drawings for BR 101-217 are dated 1930 and all steel was specified as "Structural O.H. Steel" on the drawings, which stands for open hearth steel, and was taken to be ASTM A7 (ASTM 1924) with a specified yield stress of 207 MPa (30 ksi) given the 1930 vintage (Brockenbrough 2002). Figure 3-5shows a photograph of the bridge and Figure 3-6 shows a schematic of half with the naming convention for the nodes. Note that the bridge is symmetric about the center of the span.

Figure 3-5 Photo of BR 101-217

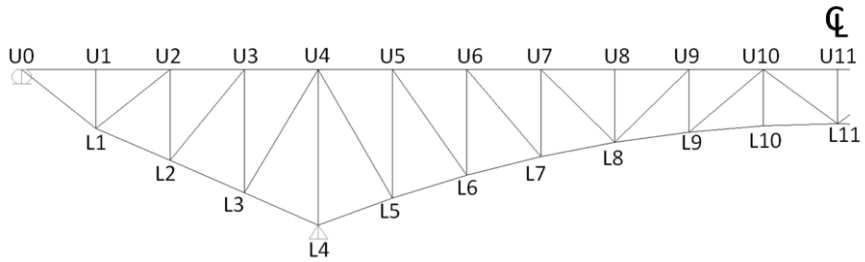

Figure 3-6 Schematic of BR 101-217

A pin support was assigned to node L4 and a roller support was assigned to node U0 consistent with the drawings. Boundary conditions were symmetric, so similar support types were assigned to the support nodes for the other half of the bridge. Similar to BR 31-36, BR 104-217 has a drop-in simple span that requires the need for an expansion joint. This joint is accommodated by sliding pin assemblies, as described above. These assemblies are located on the members spanning between nodes L8-L9 and U9-U10. Loads from the road deck are transferred from floor beams spanning between the main trusses to the panel points along the top chord and are modeled as point loads at the bridge nodes. Dead loads along the bottom chord attributed to wind bracing or other structural members are also modeled as point loads at the nodes.

3.4 Bridge and Joint Loads

3.4.1 Bridge Dead and Live Loads

Design drawings for the bridges were carefully examined to determine the appropriate dead loads for the global bridge models. As noted above, the road deck on all three bridges in question is carried by floor beams spanning transverse to the main bridge trusses. Loads from the road deck are distributed to the floor beams based on their tributary areas and then the reactions from the floor beams are transferred as point loads to the truss nodes. Dead loads from the wind bracing and other structural elements were also distributed to their appropriate nodes. Unit weights for the structural steel and concrete used in the dead load determination were 490 $\frac{lb}{ft^3}$ and 150 $\frac{lb}{ft^3}$, respectively. In addition to the road deck shown in the design drawings, WSDOT recommended adding a 1.5 in. thick layer of latex modified concrete as a wearing surface. This was applied to BR 90-134N and BR 31-36 only.

The live loads determined for each bridge correspond to the HS20 truck and HS20 lane load as described in Chapter 13 of the WSDOT Bridge Design Manual (WSDOT 2006) and shown in Figure 3-7. The HS20 truck load consists of three point loads that are representative of a three-axle truck with the location of the trailing axle being variable so that it will produce the largest possible loads on the bridge. For each truss member, the HS 20 truck is positioned to cause the maximum axial load on that member. The HS20 lane load consists of a distributed load of 640 $\frac{lbs}{ft}$ and two different point loads, only one of which is applied for each truss bridge member. The first point load is an 18 kip load associated with moments, known as the moment rider, and the second point load is a 26 kip load associated with shear, known as the shear rider. In a truss bridge the moments are carried by the chord members and the shear is carried by the web members. Thus, for chord members the HS20 lane load is calculated by using the distributed load

in combination with the moment rider. Similarly, for web members the HS20 lane load is a combination of the distributed load and the shear rider. The distributed load and the appropriate point load are positioned along the bridge to cause the maximum axial force in a particular truss member.

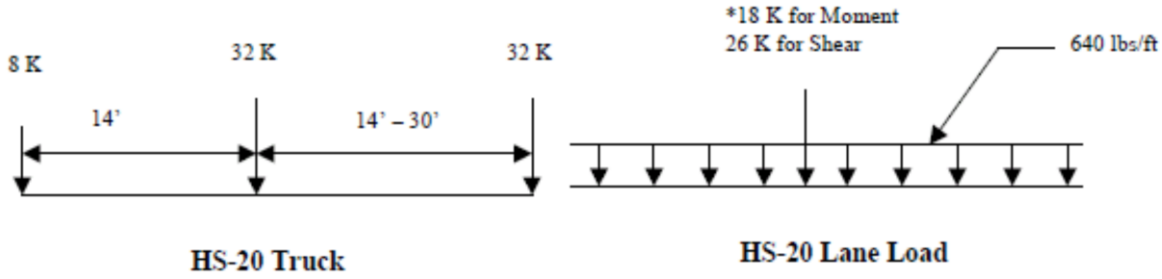

Figure 3-7 HS-20 Live Loading

3.4.2 Joint Load Cases

As many as five truss members may be connected to a single gusset plate joint. For each of those members the maximum axial force may occur with different positioning of the HS-20 live load (either the truck or lane load). Thus, for every truss joint there are as many concurrent load cases as there are members connected to the joint, where a concurrent load case is one that is in equilibrium and has a single live load position that produces a maximum axial force in at least one of the connected truss members. These concurrent load cases will be used as the loading for detailed analysis discussed in the next section.

3.5 Global Model Verification

After the Sap2000 models of the bridges were completed and the loads were determined, a comparison was made between the loads from the stress sheets from the original design drawings to those produced from analysis. Because the live loads used in the original bridge design were not necessarily the same as the HS20 live loads, model verification was done by comparing only the dead loads. The comparison showed that the truss member axial forces from the global bridge analyses closely matched the values on the stress sheets. For BR 90-134N, the largest percent difference was 3.5% for a non-hanger member. Because the hangers are lightly loaded, a small difference in axial load produced a large percent difference for those elements. For BR 31-36 and BR 101-217, the largest differences for non hanger members were 7.5% and 6.8% respectively. Therefore, the global models seem adequate for assessing truss member forces for use in evaluating selecting joints for detailed analysis.

3.6 Joint Selection

One joint from each bridge was selected for detailed finite element analysis. The selected joints had a combination of unique geometry and relatively large Whitmore section stresses associated with at least one member. Each selected joint is described in detail below and the Whitmore section stresses discussed are for factored loads at the Strength I Load Combination per AASHTO (2007).

Joint L2 from BR 90-134N was selected for detailed analysis as it had the largest Whitmore section stress of any joint on the bridge of 131.6 MPa (19.1 ksi) at the end of member L2-L4. As shown in Figure 3-8 the joint has two 13 mm (1/2 in.) thick gusset plates located on the outer faces of the members that were specified as silicon steel and taken to be ASTM A94-46 steel (ASTM 1946), for which a specified yield stress of 310 MPa (45 ksi) was assumed. Both tension and compression diagonals (L2-U3 and L2-U1 respectively) are built-up box sections as are the tension chords (L0-L1 and L2-L3), and the hanger is a built-up I-shape. The gusset also serves as a chord splice, where the splice is offset from the midpoint of the gusset, with the connection for Chord L2-L4 being longer. A floor beam is attached through a riveted web angle connection and there is a 9.5 mm (3/8 in.) thick silicon steel gusset plate at the bottom flange of the chords for attachment of wind bracing that also acts as part of the splice between the tension chords. An additional 9.5 mm (3/8 in.) thick silicon steel splice plate connects the top flanges of the chords.

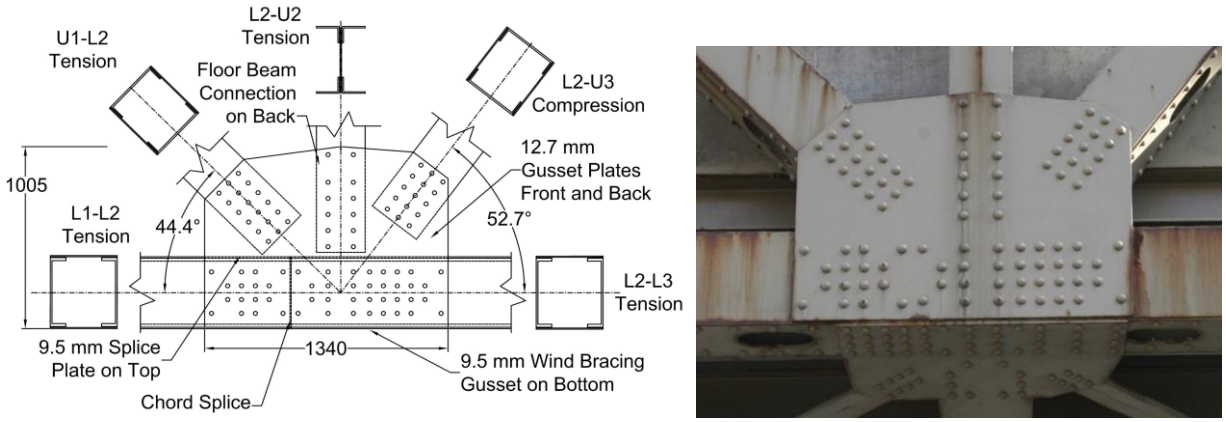

Figure 3-8 Joint L2 from BR 90-134N

Joint L9 from BR 31-36 was also selected for detailed analysis as it had a relatively large stress of 95.8 MPa (13.9 ksi) at the Whitmore section of member L7-L9 and a unique geometry as shown below. Joint L9 has two 13 mm (1/2 in.) thick gusset plates that are riveted to the outer faces of the truss members. This connection is at a hinge location in the truss and has a zero force chord

member attached (L9-L10) with a large pin along where secondary plates increase the bearing strength of the pin hole for construction loads. The loaded chord is a compression member (L7-L9) and has a built-up box cross-section composed of channels with riveted top and bottom plates. There are 13 mm thick (1/2 in.) splice plates on both sides of Chord L7-L9 that help connect it to the gusset plates. The compression diagonal (L9-U10) is also a built-up box section, the tension diagonal (L9-U8) is a built-up I-shape of angles and plate, and the vertical hanger is a rolled W12x53. Wind bracing is connected via a gusset plate attached to the bottom flange of the loaded chord member and via angles that are riveted to the gusset plates. All steel for this bridge was specified as A7 with a specified yield stress of 228 MPa (33 ksi).

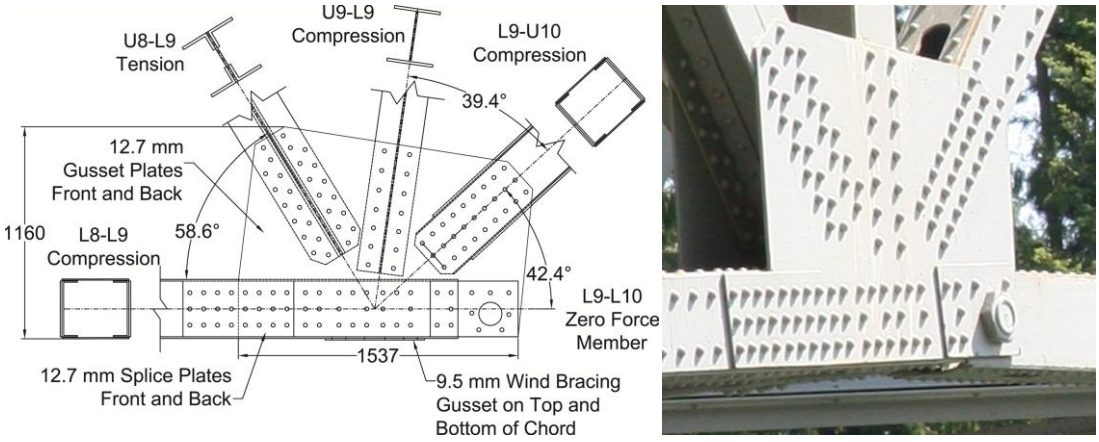

Figure 3-9 Joint L9 from BR 31-36

Joint L5 from BR 101-217 was selected for detailed analysis as it had somewhat large stresses at the Whitmore Section of the chords but also very different geometry as shown in Figure 3-10. As shown, L5 is a lower chord connection with a single I-shaped tension diagonal (L5-U4), I-shaped compression vertical (L5-U5), and built-up compression chords that are composed of channel sections (L4-L5 and L5-L6) back-to-back at a distance of approximately 280 mm (11 in.). The chord channels are stitched together with lacing away from gusset plates and solid end plates adjacent to the gusset connections. The 9.5 mm (3/8 in.) thick gusset plates are positioned between the back-to-back channels and the diagonal and vertical members pass between the gusset plates with the vertical member extending through to the bottom flange of the chord, which is the distinguishing feature for this joint. All truss members are riveted to the gusset, and therefore the compression diagonal is also riveted to the chords. Wind bracing is present at this location with transverse gusset plates attached to the top and bottom flanges of the inner channel of the chord. The chord is spliced at the midpoint of gusset and additional splice plates are present on the outer webs of the channels. Drawings indicate that the chord members were milled-to-bear

on each other. The steel is specified as "Structural O.H. Steel", which was assumed to have a specified yield stress of 207 MPa (30 ksi) as described above.

Joint U10 from the I-35 Bridge in Minneapolis shown in Figure 3-11 was also considered, since it serves as a baseline and comparison to other analytical studies. It is described in detail in Ocel and Wright (2008). The 13 mm (1/2 in.) thick gusset plates had a yield stress of 345 MPa (50 ksi) and all members were connected via rivets. This gusset was located near an inflection point in the bridge and had one chord in compression (U9-U10) and one in tension (U10-U11). Both chords were built-up box shapes and were spliced at the middle of the gusset plate. Interior 13mm (1/2 in.) splice plates were provided to connect the webs and the flange of the chords but were only attached to each chord segment via three rivet lines. The compression diagonal (L9-U10) was a built-up box shape and the tension diagonal (U10-L11) and hanger (U10-L10) were rolled I-shapes. A floor beam rested on top of the chords and wind bracing was connected to the inner gusset plate at the top and bottom of the chords via riveted angles.

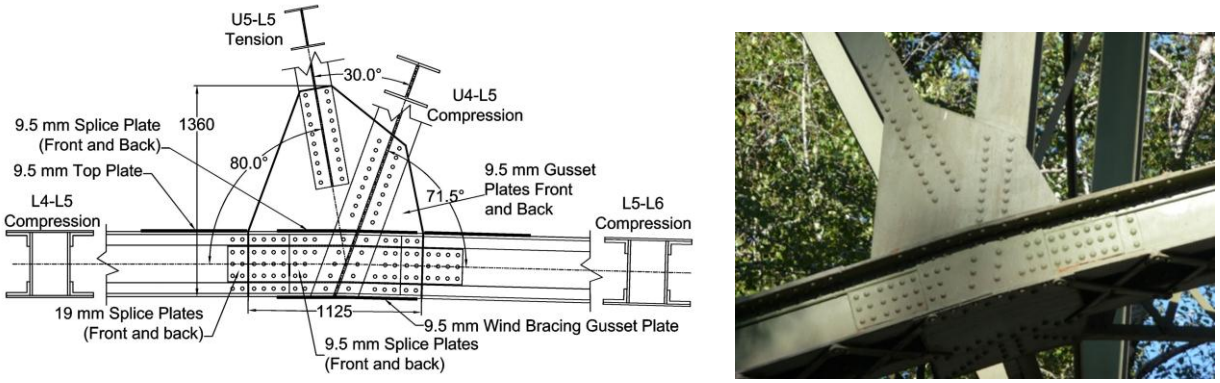

Figure 3-10 Joint L5 from BR 101-217

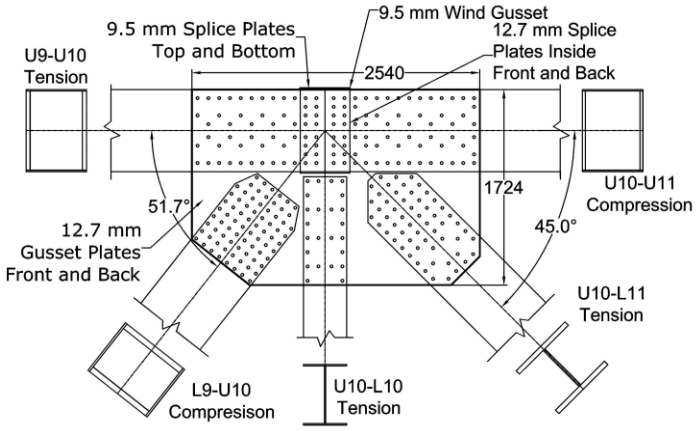

Figure 3-11 Joint U10 from I-35W in Minneapolis

Section 4 Finite Element Model Development, Validation and Implementation

4.1 Finite Element Model Development

This research uses detailed nonlinear finite element (FE) analysis of detailed models of selected gusset plates from steel truss bridges to help develop a simplified triage evaluation procedure (TEP) and compare it with the procedures in the *FHWA Guide*. As such, the development of a model of the complex gusset plate connection is necessary and the resulting models must be validated, despite the lack of experimental data. Detailed FE models of several truss bridge joints were developed using the ANSYS software package (ANSYS 2008). The development of the modeling method and verification of the method were done using Joint U10 of the I-35 Bridge and the computed results from Ocel and Wright (2008). Additional verification is provided by comparing similarly derived numerical models with prior experimental results. The modeling methods were then applied to the other joints described below.

The first step in developing the detailed models of the selected joints was to generate CAD drawings of each joint geometry. To do this, old and sometimes barely legible drawings of the bridge and bridge joints were used. Where dimensions were unclear or incomplete, assumptions were made with care taken to preserve the work point of the joints. The resulting CAD drawings provided coordinates of key points necessary for the generation of the detailed model geometries in ANSYS.

Four-noded reduced integration shell elements were used to model the gusset plates, splices, wind bracing plates and truss members in the vicinity of the gusset plates, as shown in Figure 4-1. At a distance of twice the member depth, *d*, from the gusset edge the truss members were transitioned to line elements. This distance was found to adequately model the flow of stress from the member to the gusset plates when compared with longer distances. A plane-sections-remain-plane master-slave constraint was applied at this transition. The line elements where assigned the cross-sectional properties of the truss members and ended at adjacent panel points where all degrees of freedom except translation in the member's axial direction were restrained. Thus, the restraint against gusset buckling provided by the truss members was modeled using the actual truss member cross-section and length despite the transition from shell elements to line elements. Loads were applied in the axial direction of the members at these adjacent panel points. Restraint against out-of-plane displacement of the gusset was provided at the locations where wind bracing and/or floor beams connected to the gusset.

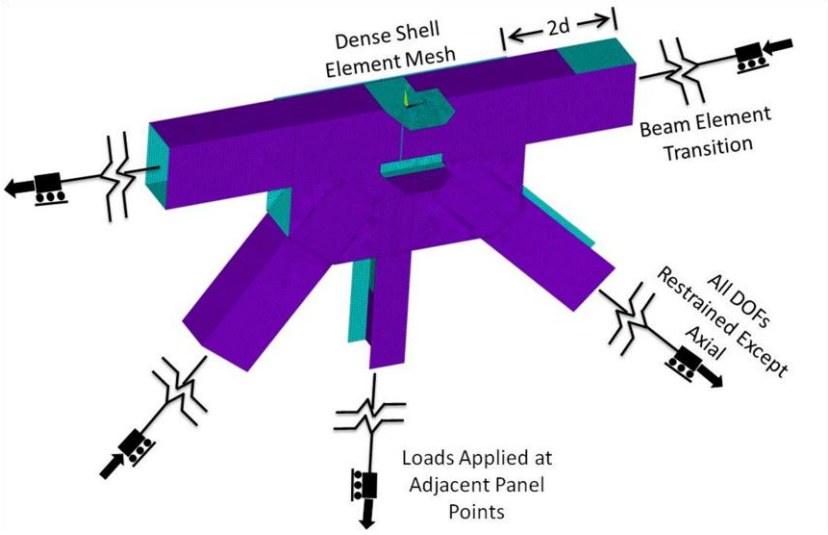

Figure 4-1 General Gusset Plate Connection Model

Other methods for applying the boundary conditions and loads were considered. These included applying loads and boundary conditions at a distance of 2*d* from the edges of the gusset plates and not including the beam element transitions. However, that approach was found to result in an unrealistic restraint of the gusset plate against out-of-plane movement and larger and possibly unconservative buckling loads. The selected approach more accurately simulated the boundary conditions for gusset plate buckling; however, the compressive load that can applied to the gusset is limited by the buckling capacity of the attached beam elements as would be expected in the bridge.

All rivets were modeled as rigid fasteners. Translational degrees of freedom of nodes at rivet locations were constrained to be equal for members and gussets plates. Contact or gap elements were not used at the surfaces, since their use greatly increases the computational time cost and complexity of analysis without significantly improving the accuracy of the prediction. This leads to conservative estimates of the gusset plate buckling load, since contact between plates and members provides additional buckling restraint which is not included with the rigid fastener method. All gusset plate and splice plate steel was modeled as bilinear kinematic hardening materials that had an initial elastic modulus of 200 GPa (29,000 ksi) and 3% strain hardening. The strain hardening was found by linearizing the stress-strain results from material tests from the I-35 Bridge gusset plate reported in Ocel and Wright (2008). All shell and beam elements modeling truss members were modeled as elastic elements so that the nonlinear response was focused upon the gusset plate response.

A mesh refinement study was conducted to determine the mesh density needed to accurately simulate the general stress field in the gusset plate. Figure 4-2 shows three mesh refinements considered, having average edge lengths of 38.1 mm (1.5 in.), 25.4 mm (1 in.) and 12.7 mm (0.5in). The Von Mises stress distributions predicted for these 3 models at the same load levels are shown in Figure 4-3. The figure shows that the overall stress distributions and magnitudes are similar for the 25.4 mm and 12.7 mm mesh densities while the 38.1 mm mesh appears to produce stress distributions that have more sharp changes. The consistency between the 25.4 mm and 12.7 mm mesh densities indicates that there is not a significant increase in accuracy for the finer mesh while the computational time was increased substantially. Therefore, 25.4 mm average element size was selected as the target for meshing the U10 gusset plate model from the I-35 Bridge as well as the other gusset plates considered. Figure 4-4 shows the resulting shell element models for the three WSDOT joints.

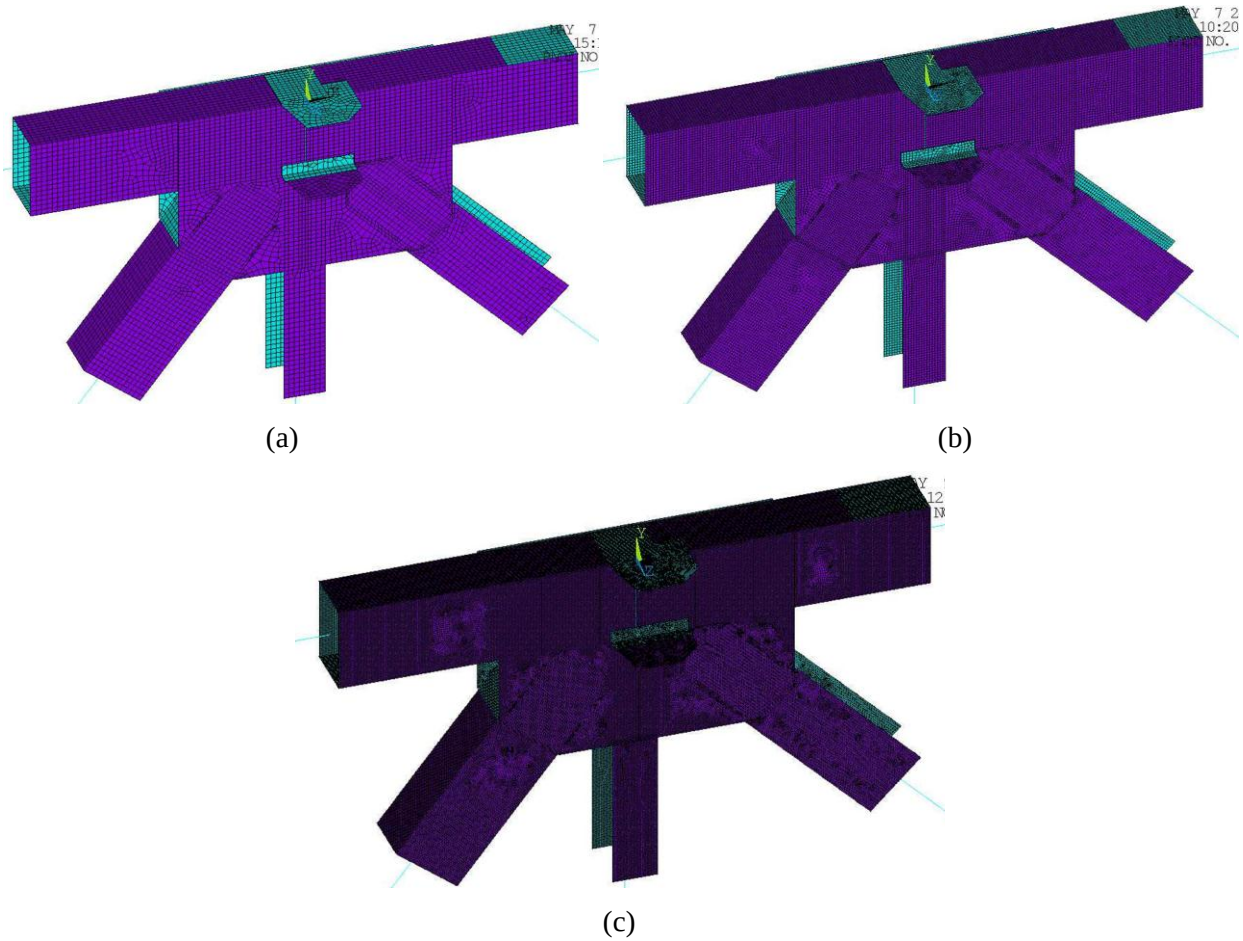

Figure 4-2 Mesh Refinements Considered: (a) 38.1 mm (1.5 in.) Average Element Edge Length, (b) 25.4 mm (1 in.) Average Element Edge Length, and (c) 12.7 mm (0.5 in.) Average Element Edge Length

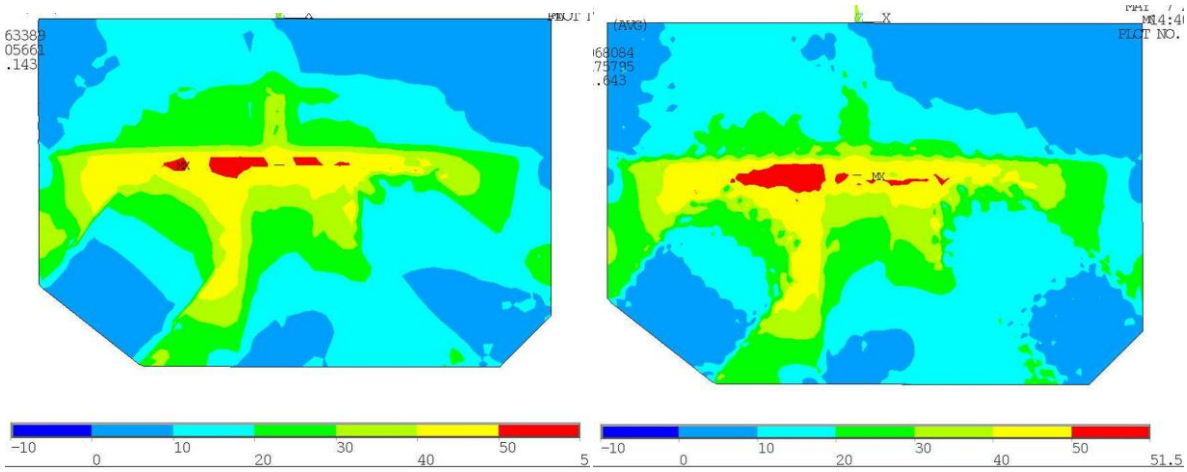

(a) (b)

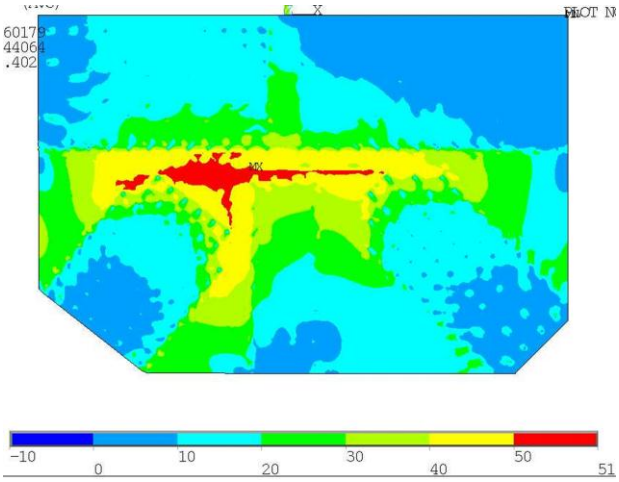

(c)

Figure 4-3 Von Mises Stress Distributions (ksi) for (a) 38.1 mm (1.5 in.) Average Element Edge Length Mesh, (b) 25.4 mm (1 in.) Average Element Edge Length Mesh, and (c) 12.7 mm (0.5 in.) Average Element Edge Length Mesh

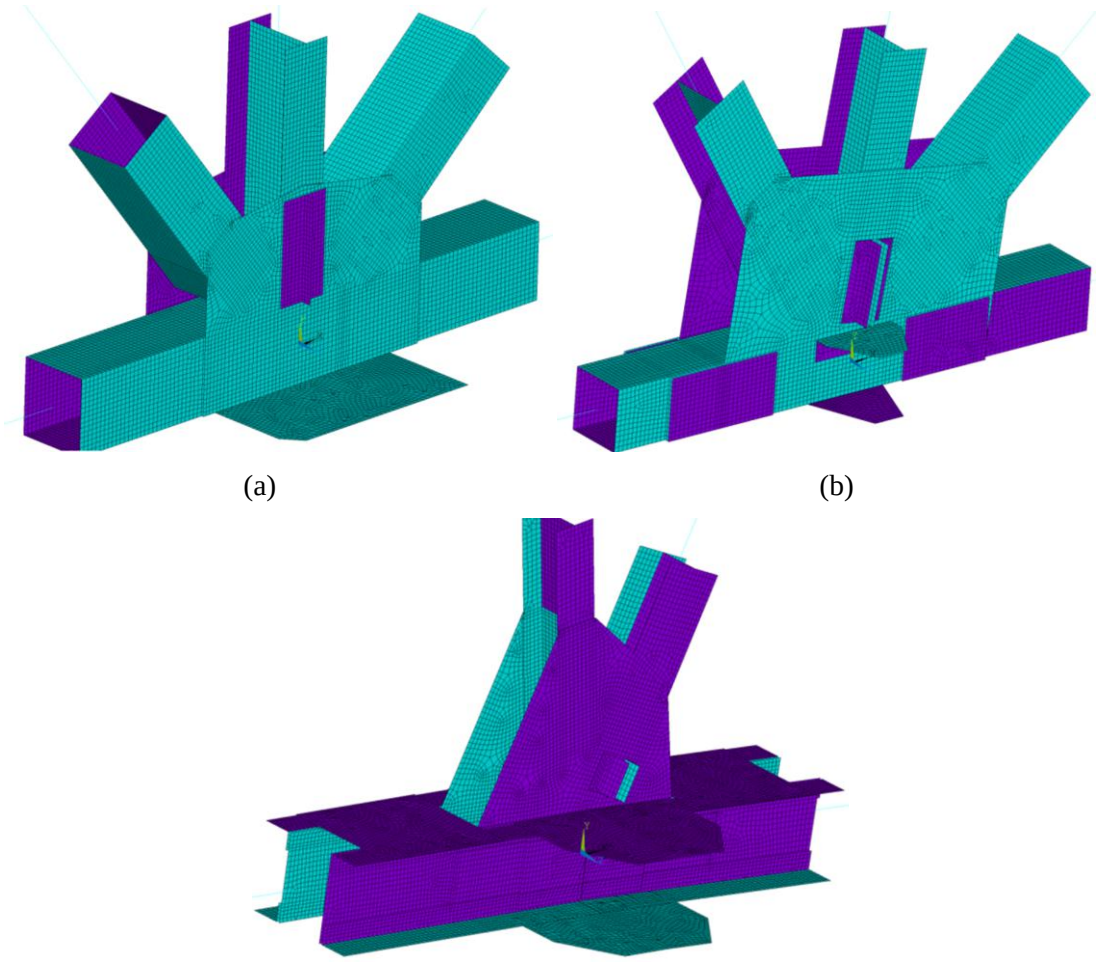

(a) (b)

(c)

Figure 4-4 Truss Bridge Joint Models (a) Joint L2 from BR 90-134N, (b) Joint L9 from BR 31-36, and (c) Joint L5 from BR 101-217.

4.2 Validation of Finite Element Models

The modeling methods described above were applied to the simulation of gusset plate connections in braced frames by Yoo et al. (2008). Similarities between those simulations and the models used here include the software, elements and material constitutive models. Yoo et al. (2008) demonstrated excellent agreement with experimental results, both in terms of global response of the braced frame system and with simulating local gusset plate stresses as shown in Figure 4-5. The figure illustrates that the regions of high stress, signified experimentally by the flaking of whitewash, match well with the areas of high stress from the simulation. It should be noted that the gusset plates in the referenced concentrically braced frames were subjected to large out-of-plane deformations as brace buckling occurred and had inelastic behavior. In the truss bridge gusset plate models developed here the analyses are kept largely within the elastic range of

behavior and the out-of-plane deformations are expected to be small. Regardless of the differences between truss bridge and braced frame gusset plates, the results in Figure 4-5 provide confidence in the ability of shell element models to capture buckling deformations and local stress distributions.

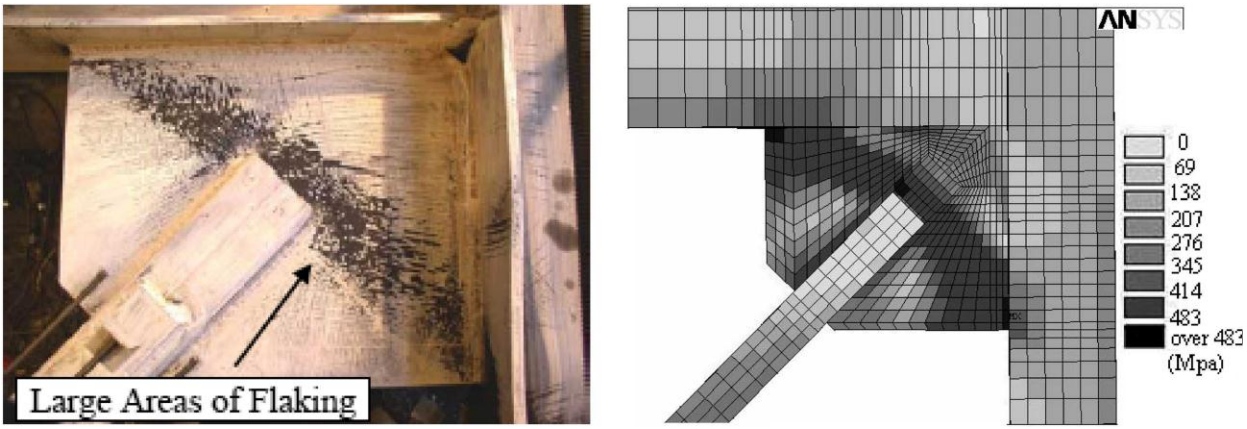

Figure 4-5 Comparison of Gusset Plate Stresses and Whitewash Flaking from Yoo et al. (2008)

To provide additional verification of the modeling techniques used here, the results of the analysis of Joint U10 from the I-35 Bridge were compared with analysis results given in Ocel and Wright (2008). In that study, the entire bridge was modeled in three-dimensions primarily using beam elements for the steel superstructure and shell elements for the deck with a detailed shell element mesh to model Joint U10. Thus the actual boundary conditions for the joint were simulated from the global bridge response. Figures 4-6 and 4-7 compare stress results for the two models under the approximate loading for the bridge at the time of collapse, as given in Ocel and Wright. Figure 4-6 compares Von Mises, shear and normal stresses along a horizontal line one element below the lower rivet line of the chord connection and shows reasonable agreement. Figure 4-7 compares the same stresses along a vertical line one element away from the hanger rivet line and again shows reasonable agreement. Therefore, the four gusset plate connections were simulated with these modeling procedures.

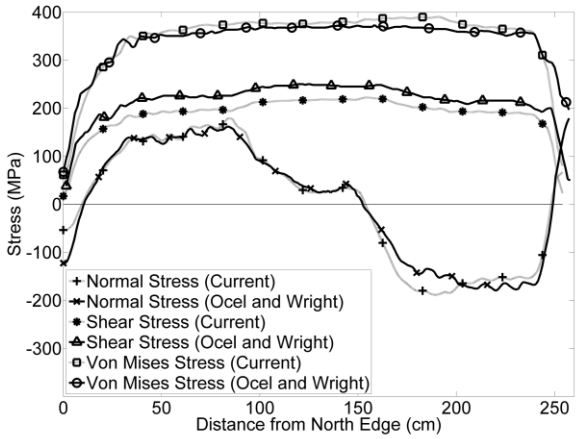

Figure 4-6 Comparison of Stresses along the Horizontal Line Just Below the Chord in Joint U10 between the Current Study and Results Reported in Ocel and Wright (2008).

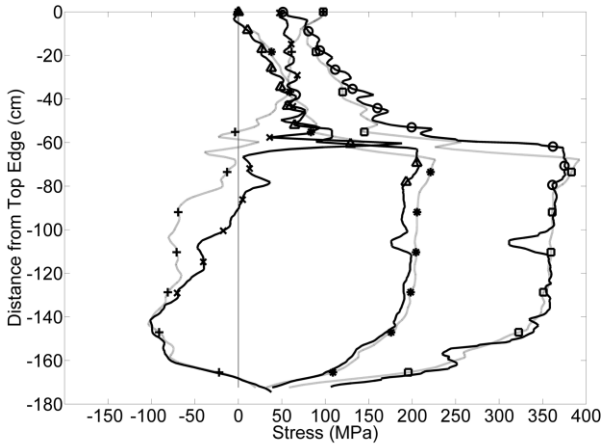

Figure 4-7 Comparison of Stresses along the Vertical Line Adjacent to the Hanger in Joint U10 between the Current Study and Results Reported in Ocel and Wright (2008).

4.3 Parameters Considered

The selected gusset plates provide considerable variation in geometry and gusset plate layout as may be encountered in practice. The distribution of load between members attached to the gusset plates and the thickness of the gusset plates were additional parameters considered in the analytical research. Gusset plate thickness was varied to establish initiation of yielding and elastic and inelastic gusset plate buckling. Gusset plate thicknesses of 3.2 mm (1/8 in.), 6.4 mm (1/4 in.), 9.5 mm (3/8 in.), and 13 mm (1/2 in.) were used for all joints except Joint L5 from BR 101-217 for which the 13 mm thickness was not considered.

A suite of load distributions for each joint was considered because of the wide variability in dynamic bridge loading and the necessity that loads satisfy equilibrium in FE analysis. These variations evaluated their impact on the stress distribution, occurrence of yielding, and buckling capacity of the gusset plates. The load distributions were determined by moving an HS-20 live load over the bridge in the global analyses and factoring the results to be consistent with the Load Factored Rating (LFR) Operating Rating Level per AASHTO (2008), including impact, and are shown in Table 4-1. The number of load distributions considered for each connection is equal to the number of truss members connected and each distribution corresponds to the concurrent loading where the axial force in a particular member is a maximum absolute value. For Joint L9 there are five members attached, one of which is a zero force member, thus there are only 4 load cases. For Joint L5 there are four members attached but only two positions of the live load are required to produce the maximum envelope loads in those members, thus there are only two load cases. For detailed connection analysis, a ramp function was used to apply continuously increasing loads to each member in a pattern that corresponds to the selected load distribution. The analysis then continues with increasing applied loads until it fails to converge due to inadequate stiffness or large deformations. It is acknowledged that different load combinations and load factors will produce different load distributions; however, the distributions used here are thought to have sufficient variation to evaluate the impact of load distribution on gusset plate behavior.

For the U10 joint from the I-35 Bridge, the load distributions were based on the estimated member forces at the time of collapse as given in Ocel and Wright (2008). Prior to calculating distributions, the reported loads at collapse were slightly adjusted such that they were in equilibrium as truss elements. This was necessary because the analysis in Ocel and Wright (2008) used fully restrained assumptions for truss member ends, but the moments and shear forces were not reported. However, the joint subassemblages modeled here required truss member forces at the ends of the line elements to be in equilibrium. The maximum change in the loads to achieve equilibrium was 4%. Each of the five load distributions for U10 was then developed by increasing the axial force in one of the five connected members by 15% and then rebalancing the other forces to maintain equilibrium. The resulting load distributions are shown in Table 4-2.

Table 4-1 Member Loads for Different Load Distribution Cases (kN)

Joint L2 (BR 90-134N)					
Load Case	L1-L2	U1-L2	U2-L2	L2-U3	L2-L3
1	2078	1214	192	-635	3325
2	2006	1464	199	-594	3404
3	2112	1431	205	-562	3465
4	1775	1281	173	-858	3199
5	2040	1359	196	-771	3474
Joint L9 (BR 31-36)					
Load Case	L8-L9	U8-L9	U9-L9	L9-U10	L9-L10
1	-2576	1994	-372	-1998	0
2	-2404	2033	-604	-1699	0
3	-2298	2005	-669	-1565	0
4	-2480	1931	-373	-1914	0
Joint L5 (BR 101-217)					
Load Case	L4-L5		U4-L5	U5-L5	L5-L6
1	-3579		931	-1153	-3022
2	-3174		1092	-1293	-2540

Table 4-2 Member Loads for Different Load Distribution Cases for U10 from I-35 (kN)

Load Case	U9-U10	L9-U10	L10-U10	U10-L11	U10-U11
1	10585	-11233	2289	9230	-2903
2	10477	-11565	2448	9373	-3318
3	9249	-10501	2522	8089	-2903
4	10205	-10637	1637	9492	-3099
5	8760	-10232	2194	8254	-3417

Section 5 Behavior of Truss Bridge Joints, Observations, and Development of the Triage Evaluation Procedure

5.1 Gusset Plate Yielding

5.1.1 Observed Behavior

Each joint analysis developed large areas of gusset plate yielding, identified as the regions where the Von Mises stress exceeds the yield stress of the gusset plate, prior to convergence failure of the analysis. An example of the progression of gusset plate yielding with increasing truss member loads is shown in Figure 5-1 for Joint U10 from the I-35 Bridge, where the contours depict the Von Mises stress and the black areas are those that have yielded. As shown, yielding begins approximately 250 mm from the end of the compression diagonal. With increasing load the yielding spreads horizontally across the gusset plate and around the ends of the diagonals. At the onset of yielding the calculated maximum Whitmore stress from any truss member was 203 MPa, 59% of the gusset plate yield stress, and as shown, yielding initiates away from the end of the diagonal. While the maximum uniaxial stress is observed at the end of the connected member, in agreement with the observation of Whitmore (1952), yielding is controlled by a biaxial stress state involving the interaction of stresses from the members. This interaction and the corresponding onset of yielding have been observed from the analyses to occur within a critical region defined by a triangle bounded by the rivet lines for the chord and hanger, and the end of the diagonal. Figure 5-1b shows the onset of gusset plate yielding occurring in this location for Joint U10.

Figure 5-1e shows the percentage of gusset plate area that is yielding relative to the axial load in the compression diagonal for Joint U10. The figure shows that once yielding begins it spreads fairly rapidly and that the onset of yielding can be reasonably approximated to correspond to yielding of 0.5% of the gusset plate area. This represents a small percentage of the total gusset plate area but a significant portion of the critical area that supports the diagonal, where yielding can cause instability resulting in inelastic gusset plate buckling. Further, yielding of this extent under service loads would be undesirable. Figure 5-2 shows 0.5% of the gusset plate area for the four joints considered in this study to demonstrate the onset of yielding as defined here.

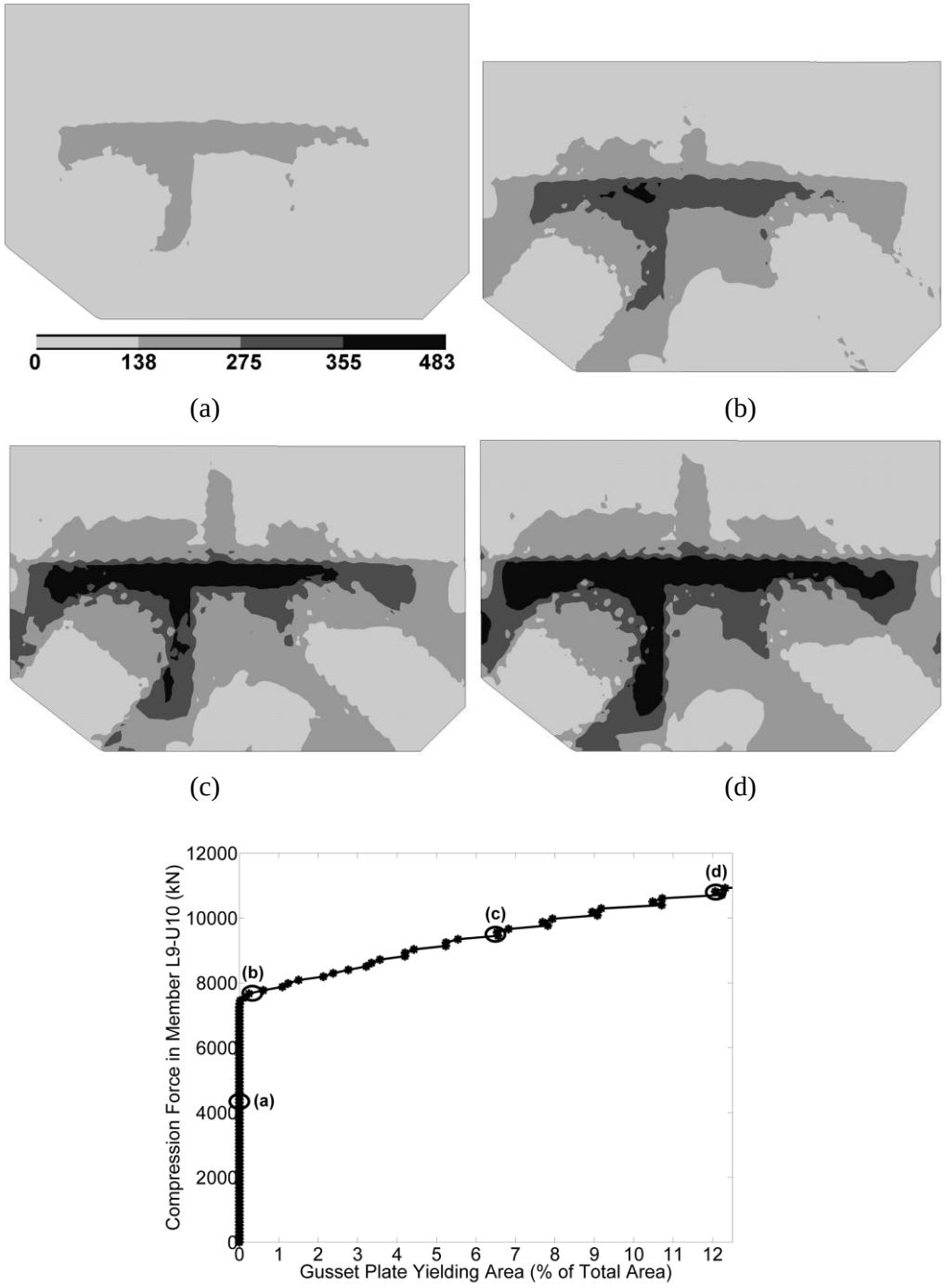

Figure 5-1 Progression of Gusset Plate with Increase in Truss Member Loads. Stress Contours Show Von Mises Stress in MPa. (a) 0% Yielded Area, (b) 0.3% Yielded Area, (c) 6.5% Yielded Area, (d) 12% Yielded Area and (e) Force in the Compression Diagonal vs. Gusset Plate Yielded Area

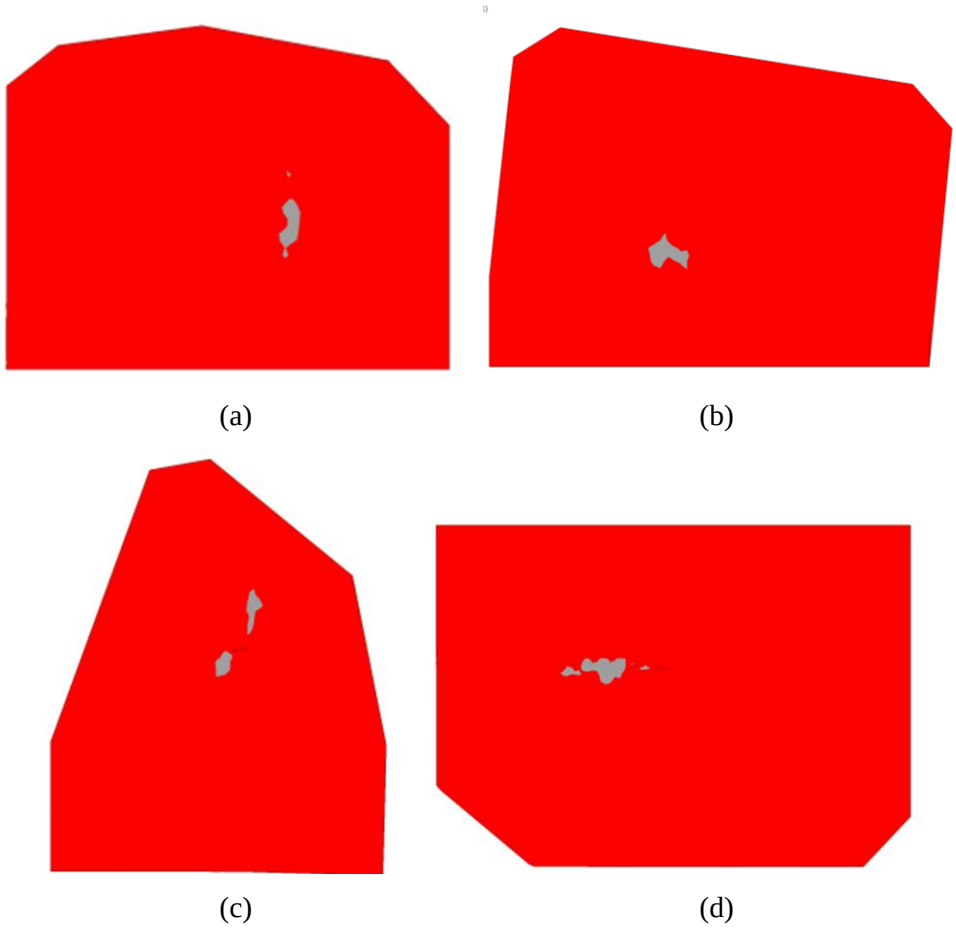

(a) (b)

(c) (d)

Figure 5-2 Illustration of 0.5% of Gusset Plate Area Yielding for (a) Joint L2 of BR 90-134N, (b) Joint L9 of BR 31-36, (c) Joint L5 of BR 101-217 and (d) Joint U10 of I-35

5.1.2 Proposed Triage Evaluation Procedure: Yielding

Yielding will in general occur prior to gusset plate failure modes such as block shear or buckling because block shear failure requires the development of stresses large enough to cause fracture and gusset plate buckling has been observed to in general be inelastic buckling. Therefore, yielding is a reasonable limit state to use for a rapid evaluation procedure. As described above, yielding in truss bridge gusset plate connections generally initiates in an interference zone as illustrated in Figure 5-3. Since the onset of yielding has been observed to occur prior to the Whitmore stress at the ends of the attached members reaching the yield stress it appears that the interactions of the stresses generated from the connected truss members must be considered. Figure 5-4 illustrates how the stresses from the two diagonal members connected to a gusset plate may interfere with each other. Here, a simple method for combining these stresses is developed. While more complex and accurate methods may be possible and are the focus of future research,

the objective of the current endeavor is to develop a conservative, simple and straightforward process for evaluating gusset plates for the onset of yielding.

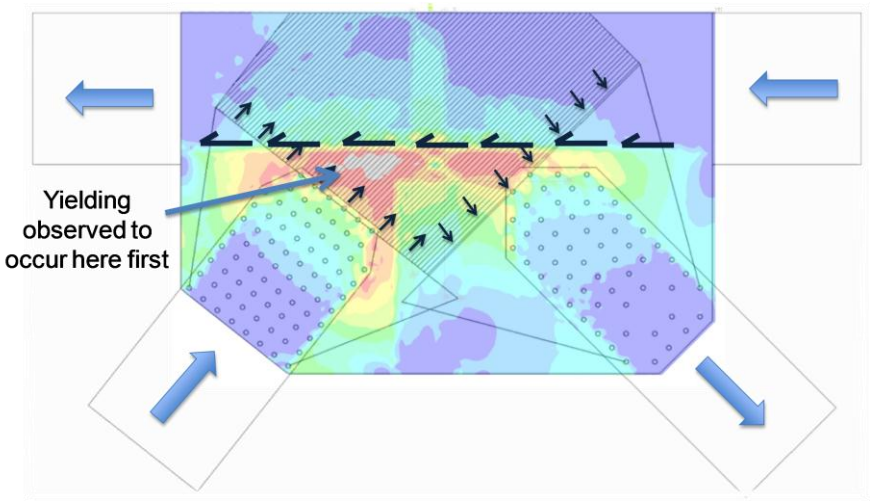

Figure 5-3 Interference of Stresses in Gusset Plate Connections

The Whitmore method conservatively predicts the maximum uniaxial stresses in the gusset at the end of a riveted member connection, which are denoted σ_{11} and σ_{22} in Figure 5-4. The TEP conservatively assumes these uniaxial stresses to be principle stresses, denoted σ_1 and σ_2, respectively. The most adverse condition occurs when these stresses for different members are orthogonal to each other and opposite in sign. Applying this assumption to the condition in Figure 5-4 results in $\theta_1 = \theta_2$, the Whitmore uniaxial stresses being principle stresses for the stress block shown, the shear stress on that stress block being zero, and the shear stress on a stress block rotated 45° from the diagonals to be the maximum shear stress. As a result, the Von Mises yield criteria for plane stress will govern yielding of the gusset:

$$\sigma_1^{\,2} - \sigma_1\sigma_2 + \sigma_2^{\,2} = \sigma_y^{\,2} \tag{3-1}$$

where σ_1 and σ_2 are principle stresses and σ_y is the yield stress. Thus, for the very worst case of σ_1 and σ_2 being equal magnitude and opposite sign, yielding will occur when $\sigma_1 = \sigma_y/\sqrt{3}$. To apply this notion to gusset plates in bridges it is necessary to determine the maximum Whitmore stress for all members intersecting the gusset, $\sigma_{w,max}$, and the proposed yield check in the TEP is:

$$\sigma_{w,\max} \le F_y \big/ \sqrt{3} \tag{3-2}$$

where F_y is the yield stress of the gusset plate.

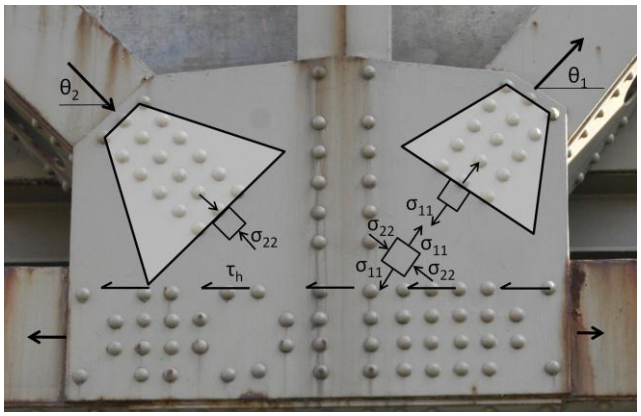

Figure 5-4 Interference of Stresses in Gusset Plate Connections

5.1.3 Comparison with the TEP and FHWA Guide: Yielding

For each analysis that did not exhibit elastic buckling (typically gusset plates above 3.2 mm (1/8 in.) thick) the truss member loads at the point in the analysis where 0.5% of the gusset plate is yielding was recorded. Those loads were then used to compute the values shown in Table 5-1, which include the maximum uniaxial stress on the Whitmore section (considering all members), $\sigma_{w,max}$, and the maximum gross shear stress (considering multiple shear sections), τ_{max} for the gusset plates at their actual thicknesses. For Joint L5 no shear stress is shown because both possible shear lines pass through either a chord or vertical hanger since the chord is continuous through the gusset and the vertical hanger passes through the gusset to the bottom of the chord as shown in Figure 3-10. Table 5-1 demonstrates that when the onset of gusset plate yielding occurs the maximum uniaxial stress on the Whitmore section and maximum shear stress are both below yield when compared to F_y and $F_y/\sqrt{3}$ values, respectively, the latter value being an approximation of the yield stress in shear. Thus, neither the shear stress nor Whitmore stress evaluations in the FHWA Guide identify the onset of gusset plate yielding. This is not surprising since the shear stress evaluation methods assume full shear yielding over the entire selected shear section and yielding along the entire Whitmore width at the end of a truss member implies that the stresses are uniaxial and are not influenced by stresses generated by other members. However, Table 5-1 does indicate that the maximum Whitmore stresses at the onset of yield are larger than or equal to $F_y/\sqrt{3}$, which is the proposed limit for the Whitmore stress in the TEP.

Table 5-1 Maximum Shear and Whitmore Stresses per the FHWA Guide at the Onset of Significant Gusset Plate Yielding

Load Distribution Case	Gusset L2 BR 90-134N		Gusset L9 BR 31-36		Gusset L5 BR 101-217		Gusset U10 I-35 Bridge	
	τ_{max} (MPa)	τ_{max} (MPa)	τ_{max} (MPa)	$\sigma_{w,max}$ (MPa)	τ_{max} (MPa)	$\sigma_{w,max}$ (MPa)	τ_{max} (MPa)	$\sigma_{w,max}$ (MPa)
1	101	101	85	140	-	133	148	237
2	114	114	82	134	-	139	149	240
3	108	108	81	132	-	-	147	243
4	111	111	85	139	-	-	153	246
5	106	106	-	-	-	-	159	256
F_y	310		228		207		345	
$F_y/\sqrt{3}$	179		132		119		199	

This is further illustrated in Figure 5-5. This figure shows Von Mises stress contours in the gusset plate of each joint for a selected load case at the onset of yield with white areas indicating locations of yielding. Shown around the perimeter of each gusset plate are the demand-to-capacity ratios (D/C) for each element found using the TEP and the element loads at this stage in the analysis, i.e., the values are the ratio of the Whitmore stress at each member end at the onset of gusset yield, divided by $F_y/\sqrt{3}$. Note that for Joint L5 the D/C ratio for the chords is 0.0 because they were specified as milled-to-bear on each other and therefore do not contribute to the stress in the gusset plate. At the bottom of each gusset plate is the D/C ratio computed using the element loads at the onset of yield as the demand and the checks in FHWA Guide as the capacity with Ω = 0.74 for shear, the most conservative value, all resistance factors as specified in the guide and the lowest D/C ratio from all limit states reported. The figure demonstrates that the TEP consistently produces D/C ratios greater than 1.0 at the onset of yielding while the FHWA guide procedure does not.

Considering the results presented in Table 5-1 and Figure 5-5, it is clear that the TEP is conservative with respect to indicating the onset of gusset plate yielding. Further, it also appears that the procedures in the FHWA Guide do not indicate the onset of gusset plate yielding. While only a single load case has been shown, similar results were obtained for all different load distributions considered.

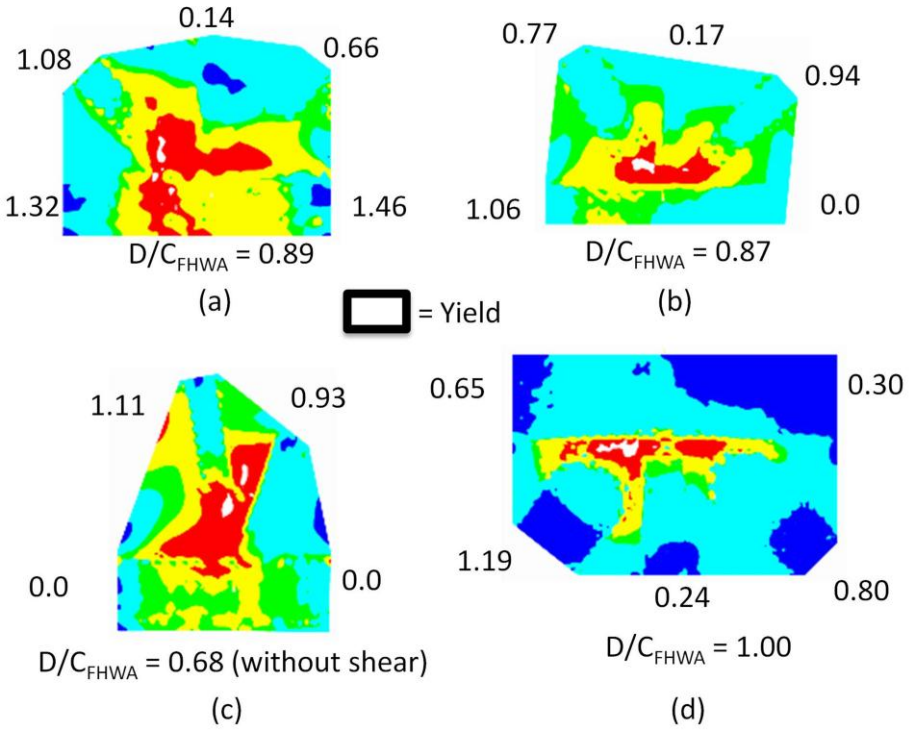

Figure 5-5 Comparison of Demand-to-Capacity Ratios for the TEP and the FHWA Guide for Load Case 1 at the Onset of Yield (a) Joint L2 of BR 90-134N, (b) Joint L9 of BR 31-36, (c) Joint L5 of BR 101-217 and (d) Joint U10 of I-35

5.2 Gusset Plate Buckling

5.2.1 Observed Behavior

Analyses were continued until gusset buckling or convergence failure of the analysis was observed. Out-of-plane restraint was provided only at the locations where lateral load bracing or floor beams were attached and at the adjacent panel points. Gusset buckling was not possible with Joint L5 because the compression member passes through the channel chords to the bottom of the gusset. Large initial imperfections were not considered; however, it was necessary to seed buckling for Joints U10 and Joint L9 with initial imperfections in the shape of the first buckling mode, found from an eigenvalue buckling analysis of the gusset plates, applied with a maximum magnitude of 1.0% of the plate thickness. In Joint L2 the floor beam load applied at the center of the rivet line attaching the floor beam web to the web angles provided adequate eccentricity in the model to initiate buckling. Figure 5-5 shows typical buckled shapes for selected gusset plate connections with deformations magnified by a factor of approximately 40. In L2, L9, and U10 a

sidesway buckling mode was observed with the compression diagonal swaying to one side of the gusset.

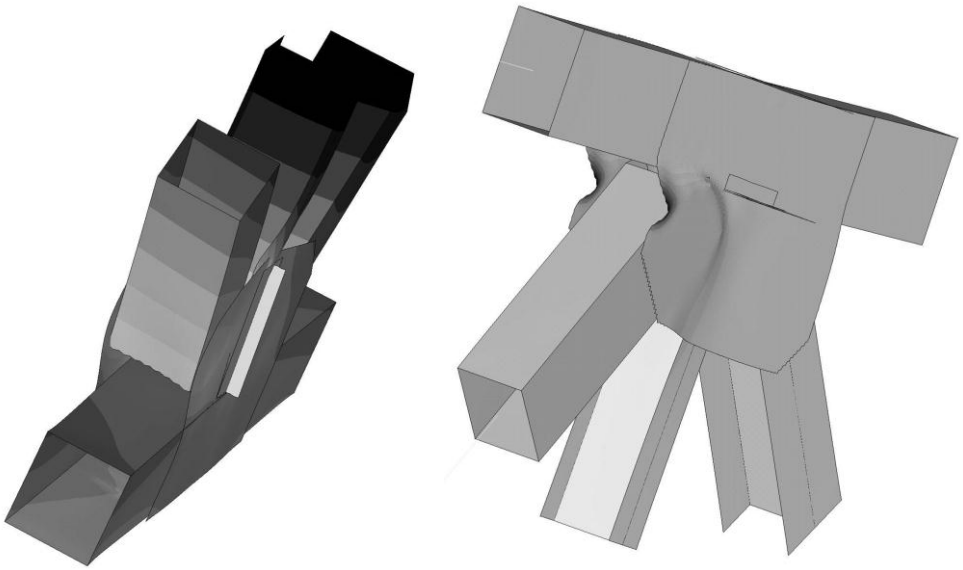

(a) (b)

Figure 5-6 Buckled Shapes of (a) Joint L2 of BR 90-134N and (b) Joint U10 of I-35

Inelastic gusset plate buckling was common and elastic buckling was observed only with extremely thin (3.2 mm [1/8 in.]) gusset plates. Where buckling was observed, the out-of-plane displacements of the gusset plate nodes at locations shown in Figure 5-7a were recorded. Figure 5-7b shows the typical progression of out-of-plane displacement along the line parallel to the compression member. Similar behavior was observed along the free edge. Since contact between the gusset plate and truss members was not modeled some of the gusset nodes deform into the truss members causing a conservative estimate of gusset plate buckling capacity. Compressive force versus maximum out-of-plane displacement was plotted for both locations of Figure 5-7a and the buckling load was conservatively taken as the load at the intersection of the initial tangent and the tangent representing 15% of the initial tangent as demonstrated in Figure 6-6. For all cases, the buckling load found using the node at the free edge and the buckling load found using the node aligned with the compression diagonal were within 5%, with the latter typically being lower and used for the buckling loads reported herein.

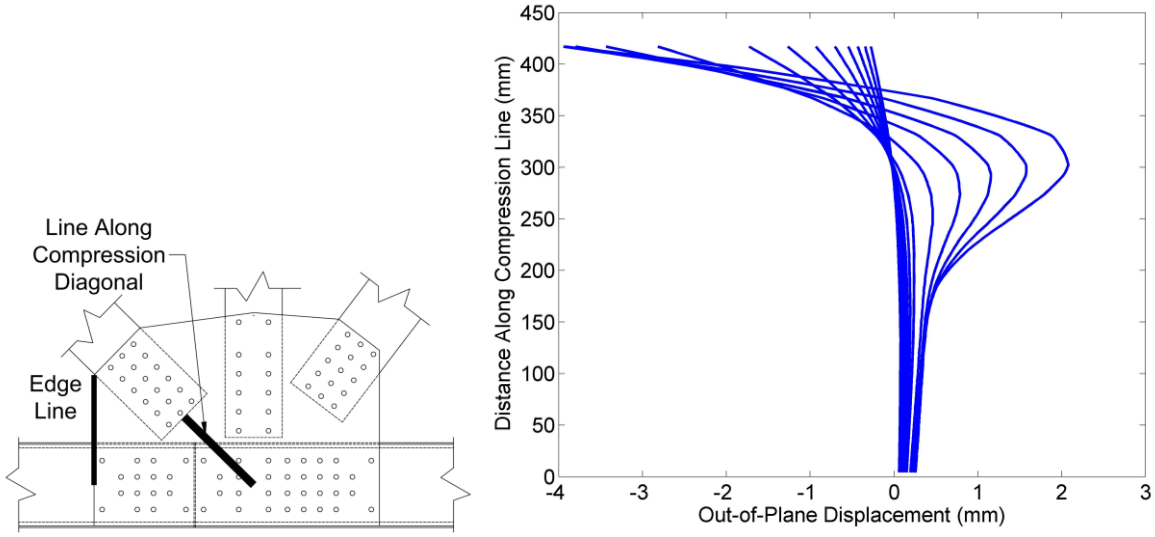

(a) (b)

Figure 5-7 (a) Lines Where Out-of-Plane Displacements were Monitored (b) Typical Progression of Out-of-Plane Displacement along the Compression Diagonal

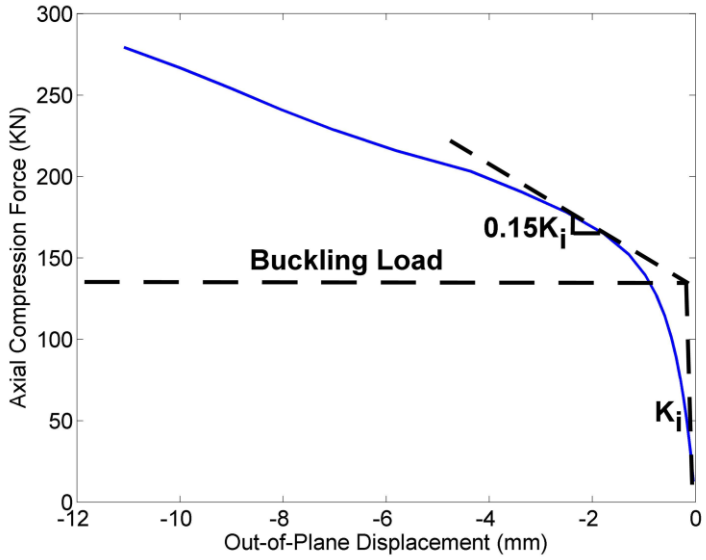

Figure 5-8 Determination of the Buckling Load from the Compressive Force versus Out-of-Plane Displacement Results

5.2.2 Comparison with Simplified Calculations for Gusset Plate Buckling Capacity

The three methods shown in Figure 2-1 for calculating the unbraced compression length and compressive stress for buckling (Thornton, Modified Thornton, and Yoo, respectively) were considered for use in calculating the gusset plate buckling capacity with the AASHTO column buckling equations (AASHTO 2007). Figures 5-9a, 5-9b and 5-9c compare the buckling strength calculated with the three methods with the buckling load established from the analyses for several different values of the effective length factor, *K*, and a yield stress of 345 MPa (the maximum yield stress for any of the gusset plates). All curves and data are shown versus *L/t*, where *L* is the unbraced length per the corresponding method and *t* is the gusset plate thickness and the observed buckling stresses have been normalized by the actual gusset plate yield stress. Each figure shows 56 data points, 20 from Joint L2 of BR 90-134N, 20 from Joint U10 of the I-35 Bridge and 16 from Joint L9 of BR 31-36. Variations in both the gusset thickness and in the load distribution were considered. Cases where global or local buckling of a truss member occurred prior to gusset plate buckling were excluded from the data and were common when the thicker gusset plates were used.

As shown in Figures 5-9a and 5-9c, the Thornton and Yoo methods appear unconservative at low values of *L/t* for any value of *K* and both result in two of three unbraced lengths used in the average unbraced length being zero for all three gusset plate configurations considered. Thus, the average unbraced length is small even when the gusset thickness is small. However, the Modified Thornton Method proposed by Yam (1994), which uses only the unbraced length aligned with the compression diagonal's centroid, is shown to be reasonably conservative in Figure 5-9b with *K* of 1.0. Based on these results, the Modified Thornton Method is recommended for calculating the unbraced length as part of the proposed TEP. Note that the gusset plates considered here displayed inelastic buckling at their actual thickness and the yield check of the TEP governed over gusset plate buckling, which is likely to be the case for most gusset plate configurations.

Buckling loads were compared to the necessary to cause the onset of gusset plate yielding. For all joints on the three WSDOT bridges with gusset plates at their design thicknesses compressive buckling loads were calculated for the gusset plates attached to the compression diagonal using the proposed method with a resistance factor, φ_P, of 0.9. When compared to the values obtained for checking the onset of gusset plate yielding per the TEP with no resistance factor, it was found that the buckling load is consistently larger than the force associated with the TEP yield check.

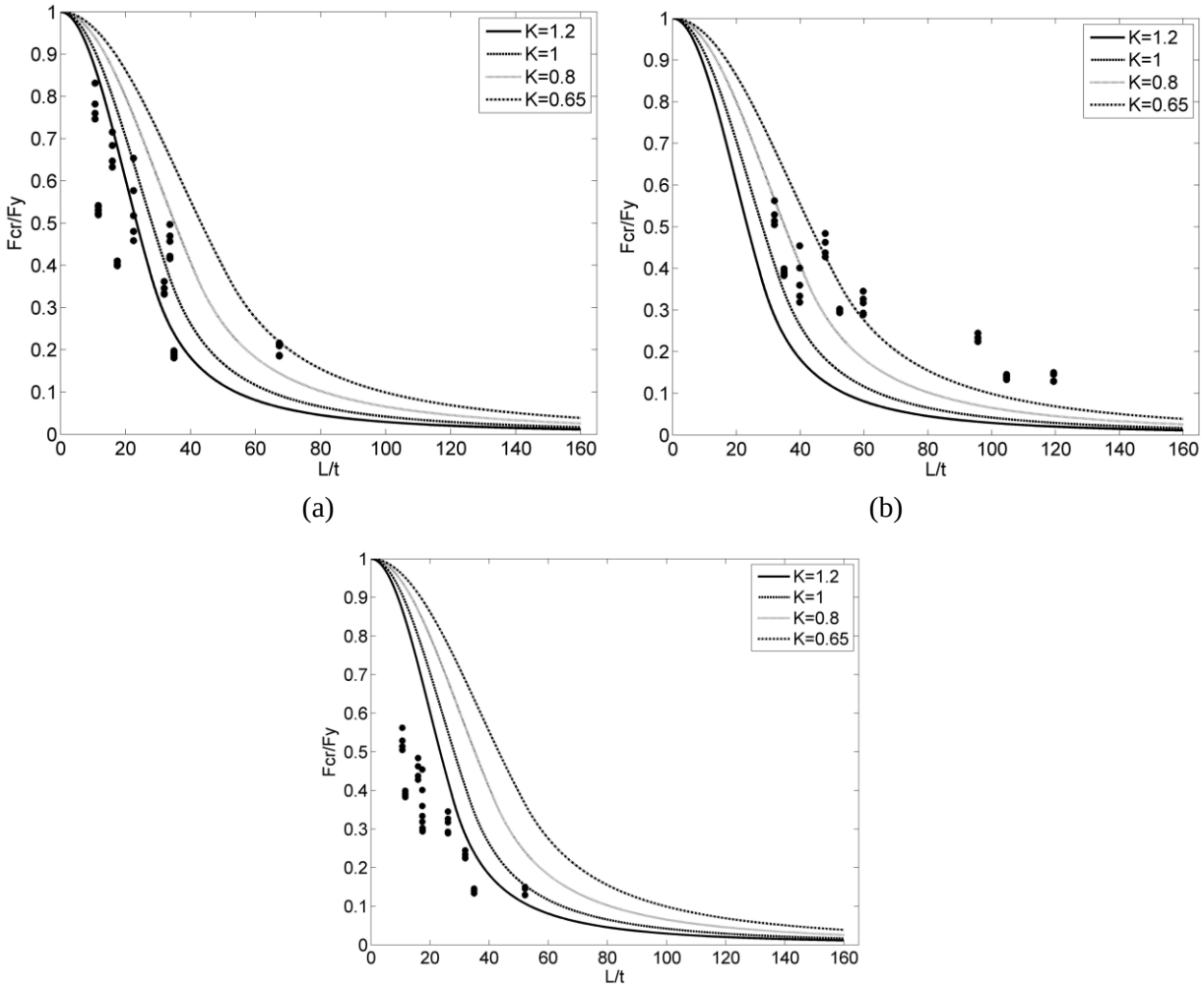

Figure 5-9 Comparison of Buckling Stress versus Effective Length from Analysis with Buckling Stress Predicted Using (a) the Thornton Method, (b) the Modified Thornton Method, and (c) the Yoo Method

5.3 Comparison of Block Shear and the TEP Yield Check

To ensure that the TEP check for the onset of gusset plate is conservative with respect block shear, a small parametric study was performed using the generalized member-to-gusset plate connection shown in Figure 5-10. Note that the connection to the gusset plate may be symmetric in the case of diagonal or hanger attachment or it may not be symmetric in the case of a chord connection. The variables defining the connection geometries are: L_{vg} = gross shear length, L_{vn} = net shear length, L_{tg} = gross tension length, L_{tn} = net tension length, n_{rt} = number of rivets along the tension line, n_{rv} = number of rivets along the shear line, d = rivets diameter, and t_p = gusset

plate thickness. Assuming that the rivets are equally spaced at a center-to-center distance that is a multiple of their diameter, αd, the connection geometry parameters may be written as:

$$L_{vg} = \alpha d\left(n_{rv} - 1\right) \tag{6-1}$$

$$L_{vn} = d\left(\alpha - 1\right)\left(n_{rv} - 1\right) \tag{6-2}$$

$$L_{tg} = \alpha d\left(n_{rt} - 1\right) \tag{6-3}$$

$$L_{tn} = d\left(\alpha - 1\right)\left(n_{rt} - 1\right) \tag{6-4}$$

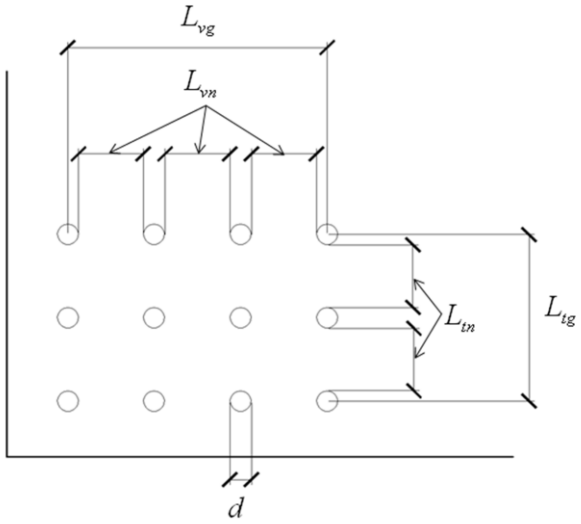

Figure 5-10 Basic Connection Geometry and Definitions

The block shear resistance of a connection is given in the FHWA Guide as:

$$\text{If } A_{tn} \geq 0.58A_{vn}, \quad \text{Then} \qquad P_r = \phi_{bs}\left(0.58F_yA_{vg} + F_uA_{tn}\right) \tag{6-5}$$

$$\text{Otherwise} \qquad P_r = \phi_{bs}\left(0.58F_uA_{vn} + F_yA_{tg}\right) \tag{6-6}$$

where ϕ_{bs} is 0.8. For the failure surface shown in Figure 5-11a and considering Eqs. 6-1 through 6-4, the block shear strength of the connection may be re-written as:

$$\frac{P_r}{t_pd} = \phi_{bs}\left[\left(0.58F_y\alpha\left(n_{rv} - 1\right) + F_u\left(\alpha - 1\right)\left(n_{rt} - 1\right)\right)\right] \tag{6-7}$$

$$\frac{P_r}{t_p d} = \phi_{bs}\left[\left(0.58F_U\left(\alpha-1\right)\left(n_{rv}-1\right)+F_u\alpha\left(n_{rt}-1\right)\right)\right] \tag{6-8}$$

where the small section indicated in Figure 5-11a have been conservatively negelected. Similarly, considering the Whitmore section shown in Figure 5-11b, the TEP yield force may be written as:

$$\frac{P_r}{t_p d} = \frac{\left[\left(n_{rt}-1\right)+\left(n_{rv}-1\right)tan30°\right]\alpha F_y}{\sqrt{3}} \tag{6-9}$$

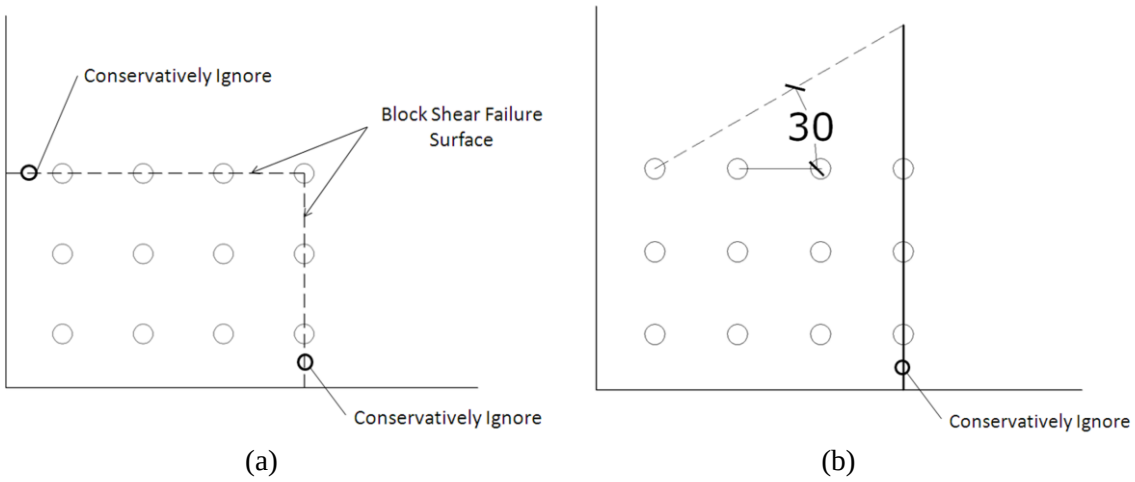

Figure 5-11 (a) Block Shear Failure Surface for Chord and (b) Whitmore Section for Chord Used for TEP Stress Calculation

Eqns (6-7), (6-8) and (6-9) are then used to compare the resistance calculated from block shear to that calculated from the TEP yield check. Figure 5-12 shows the ratio of block shear capacity to the TEP yield strength for a reasonable range of connection parameters and material strengths. Note that ASTM specification through 1949 specified that the yield stress, F_y, be ½ the tensile stress, F_u, for structural steel while also meeting an additional specified lower bound (Brockenbrough 2002). Thus, the range of the ratio F_u/F_y considered in Figure 5-12 is adequate. Further, it has been observed from various truss bridge joint drawings that the spacing of the rivets is not likely to be less than 3*d*. Therefore, the values of α considered (3 and 4) are representative of the likely values as well. As Figure 5-12 shows, block shear strength is never less than the TEP yield strength.

The same process was followed for block shear failure surfaces and Whitmore sections typical of a diagonal or hanger connection as shown in Figure 5-13. The ratio of block shear strength to

TEP yield strength for this configuration and the same parameters considered above is shown in Figure 5-14. As shown, the block shear strength is always larger than the TEP yield strength. This section has demonstrated that the TEP yield strength is conservative relative to block shear for the range of connection parameters expected in truss bridge joints.

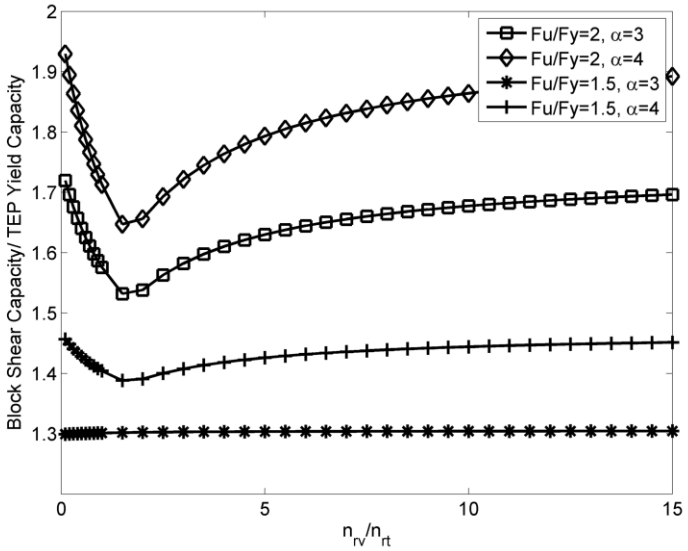

Figure 5-12 Ratio of Block Shear Strength to TEP Yield Strength for Chord Connections and Various Connection Parameters

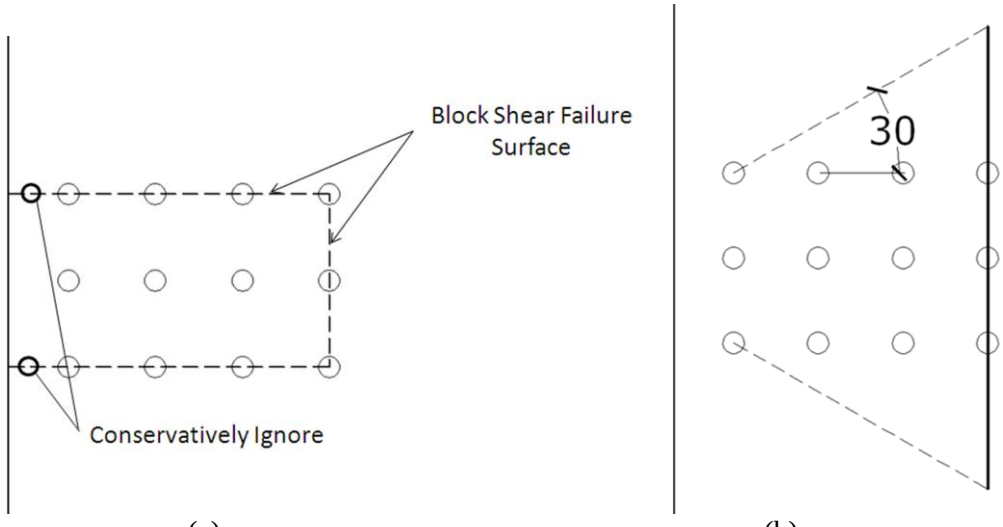

Figure 5-13 (a) Block Shear Failure Surface for Diagonal or Hanger and (b) Whitmore Section for

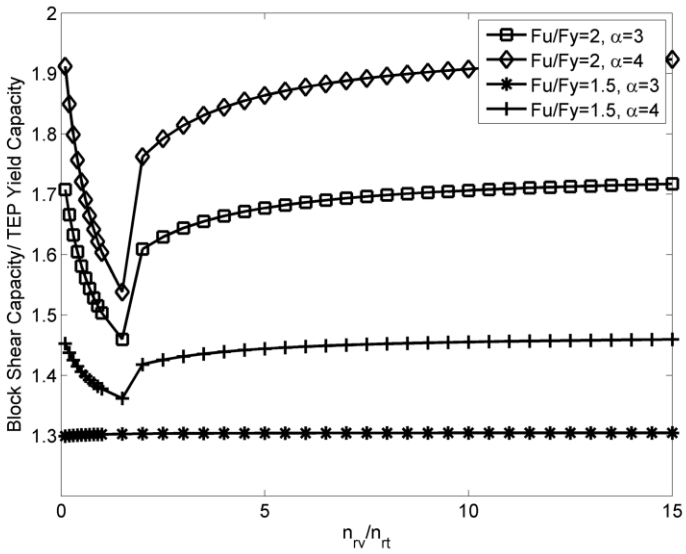

Figure 5-14 Ratio of Block Shear Strength to TEP Yield Strength for Diagonal or Hanger Connections and Various Connection Parameters

Section 6 Application of the TEP

6.1 General

As described above, the TEP consists of three primary checks, namely, gusset plate yielding, gusset plate buckling and fastener strength. Here, the fastener strength is not considered and is instead discussed in Section 8. Therefore, the following recommended checks are applied to truss bridge joints as part of the TEP in this section:

1. *Gusset plate compression and tension yielding*: Compare the maximum Whitmore stress, using a 30° dispersion angle, from any connected member with $F_y/\sqrt{3}$, where F_y is the yield stress of the gusset.
2. *Gusset plate buckling:* The buckling equations in the AASHTO LRFD (AASHTO 2007) are recommended for evaluating gusset plate buckling with an effective length factor, *K*, of 1.0. The Modified Thornton Method by Yam (1994) is recommended for establishing the unbraced length and the gusset section properties, where the unbraced length is taken as the distance from the end of the compression member connection to the next line of gusset plate support (typically a gusset-to-chord connection rivet line) and a 45° dispersion angle is used.

6.2 Joint U10 of I-35W

Prior to applying the TEP to the selected WSDOT bridges it was applied to Joint U10 of I-35W as this joint should be identified as a problem joint in the TEP as it has been shown to have been overstressed by this analytical study and others (Ocel and Wright 2008). Three loading conditions from Ocel and Wright (2008) were considered for Joint U10: (i) the loads denoted Step 2 that are an estimate of the forces due to the dead loads when the bridge first opened for service, (ii) the loads denoted Step 3 that are an estimate of the forces due to the dead loads after modifications were made to the bridge in 1999 and (iii) the estimated loads at the time of collapse. Table 6-1 shows demand-to-capacity ratios (DC ratios) for these three loading conditions for Joint U10, where the demand is the maximum Whitmore stress considering all members and the capacity is $F_y/\sqrt{3}$ per the TEP. As shown in Table 6-1 the DC ratio is 1.04 for the Step 2 loading, which indicates this gusset plate was likely to be yielding under only dead loads when the bridge opened for service. With the addition of the construction and traffic loads estimated to be on the bridge at the time of collapse the DC ratio climbs to 1.42 for the TEP. Gusset plate yielding at both load levels has indeed been confirmed by finite element analyses conducted as part of this research

and by those conducted by Ocel and Wright (2008). DC ratios are also shown for the limit states in the FHWA Guide with resistance factors per the LRFR procedure. For the three loading conditions the horizontal shear governed the capacity of the gusset plate with the factor Ω taken as 0.74 (see the FHWA Guide), resulting in DC ratios above 1.0 for both Step 3 and 4 loads. The values indicate the TEP is conservative relative to FHWA Guide.

Table 6-1 Demand-to-Capacity Ratios for Joint U10 of I-35 for Load Steps 2, 3, and 4 from Ocel and Wright (2008)

	Step 2 (Dead Loads 1965)	Step 3 (Dead Loads 1999)	Step 4 (Loads at Collapse)
TEP	1.04	1.29	1.42
FHWA Guide	0.98	1.20	1.29

6.3 WSDOT Bridges

6.3.1 TEP Load Ratings

The TEP was applied to the three WSDOT bridges to assess the relative conservativeness of the procedure. Rating factors (RFs) were computed three ways: (i) per the load and resistance factor rating (LRFR) method in the AASHTO Manual for Bridge Evaluation (AASHTO 2008), denoted the MBE herein, (ii) per the load factor rating (LRF) method in the MBE and (iii) per the LRFR method in Chapter 13 of the WSDOT Bridge Design Manual (WSDOT 2010). In all cases the HS-20 live load described above was used with only a single truck considered at one time for the truck load, the lane applied to cause the maximum effect in the 2D truss model and no lane load reductions considered. For the LRFR method in the MBE the $RF_{MBE\text{-}LRFR}$ is computed as:

$$RF_{MBE-LRFR} = \frac{\phi_c \phi_s \phi R_n - \gamma_{DC} DC - \gamma_{DW} DW}{\gamma_{LL}\left(LL + IM\right)} \tag{6-11}$$

where ϕ_c is the condition factor, taken as 0.95 here, ϕ_s is the system factor, taken as 0.9 here, ϕ is the LRFD resistance factor, R_n is the nominal resistance, *DC* is the components dead load, *DW* is the wearing surface dead load, *LL* is the live load, γ is the load factor for particular load, and *IM* is the dynamic effect of the live load taken to be 1.33 here. The load factors are given in Table 6-2. Note that the MBE allows for LRFR at the both the strength and service limit states each at inventory or operating load levels. Different load factors are given for each of these as shown in Table 6-2, where only the Strength I and Service II limit states are considered here. While RFs

are computed for all four combinations of limit state and load level, the Service II limit state is suggested for use with the TEP because the yielding check is not a failure mode, but rather indicates the onset of yielding and in all cases considered here the yielding check governed over the compression buckling check.

Table 6-2 Load Factors for Load Rating with Different Load Rating Procedures

	MBE – LRFR			
	Strength I		Service II	
Load Factor	Inventory	Operating	Inventory	Operating
γ_{DC}	1.25	1.25	1.0	1.0
γ_{DW}	1.5	1.5	1.0	1.0
γ_{LL}	1.75	1.35	1.3	1.0
Load Factor	MBE – LFR			
	Inventory		Operating	
A_1	1.3		1.3	
A_2	2.17		1.3	
Load Factor	BDM – LRFR			
γ_D	1.2			
γ_L	1.8			

For the LFR method in the MBE, which is the same as the National Bridge Inventory Rating in the WSDOT Bridge Design Manual, the $RF_{MBE\text{-}LFR}$ is computed as:

$$RF_{MBE-LFR} = \frac{C - A_1 D}{A_2 L(1+I)} \tag{6-12}$$

where C is the capacity, A_1 is the load factor for dead loads, A_2 is the load factor for live loads, D is the dead load, and L is the live load. I is the dynamic impact factor which is given by:

$$I = \frac{50}{125 + L} \tag{6-12}$$

where L is the length in feet of the portion of the span that is loaded to produce the maximum stress in the member with a maximum value of 0.3. The load factors are given in Table 6-2 for

both inventory and operating load levels. For the LRFR method from the WSDOT Bridge Design Manual (BDM), the $RF_{BDM\text{-}LRFR}$ is calculated as:

$$RF_{BDM-LRFR} = \frac{\phi R_n - \gamma_D D}{\gamma_L L(1+I)} \tag{6-13}$$

where ϕ is the resistance factor per the 1989 AASHTO *Guide Specifications for Strength Evaluation of Existing Steel and Concrete Bridges* (AASHTO 1989), R_n is the nominal resistance, D is the dead load, L is the live load, I is the dynamic impact factor is taken as 0.2 here and γ is the load factor for particular loads which are shown in Table 6-2. Note that the $RF_{BDM\text{-}LRFR}$ is defined only at the strength limit state and no distinction between the inventory and operating load levels is made.

Tables Table 6-3 through 6-5 show the rating factors for the joints of the three bridges found using the three different approaches with the TEP and neglecting the rivet checks. Joints with only hanger connections are not included. As shown, the TEP results in a number of RF's less than 1.0 when used with MBE LRFR method with the Strength I load combination at the inventory load level. This is because this is a strength load combination and the TEP is based on the onset of yield. Examining the RFs for the MBE LRFR method with the Service II load combination at the inventory load level indicates that at service loads, 2 out the total of the 35 joints may be yielding under service loads and would require additional investigation. These joints are discussed in more detail below. At the operating load level using the MBE LRFR method none of the RFs are less than 1.0 for the Service II load combination while several are less than 1.0 for the Strength I load combination.

The joints with RFs less than 1.0 from the MBE LFR method at the inventory load level are similar to those with RFs less than 1.0 for the MBE LRFR method with the Strength I load combination at the inventory load level. However, the RF's are generally larger for the LFR method. One joint has an RFs less than 1.0 for the MBE LFR method at the operating load level and for the BDM LRFR method only four joints have RFs less than 1.0.

Table 6-3 Rating Factors for BR 90-134N Joints Using the TEP

	MBE - LRFR Strength I		MBE - LRFR Service II		MBE - LFR		BDM - LRFR
Joint ID	Inventory	Operating	Inventory	Operating	Inventory	Operating	
L2	1.34	1.73	2.20	2.86	1.60	2.67	2.03
L4	1.19	1.54	2.00	2.60	1.44	2.41	1.84
U1	1.49	1.93	2.33	3.03	1.58	2.63	2.15
U3*	0.75	0.97	1.41	1.84	0.99	1.66	1.29

* Indicates joints where all RFs would be greater 1.0 if compressions chords that are milled-to-bear were neglected.

Table 6-4 Rating Factors for BR 31-36 Joints Using the TEP

	MBE - LRFR Strength I		MBE - LRFR Service II		MBE - LFR		BDM - LRFR
Joint ID	Inventory	Operating	Inventory	Operating	Inventory	Operating	
L1	0.75	0.97	1.13	1.46	0.94	1.56	1.15
L3	1.15	1.50	1.82	2.36	1.58	2.64	1.88
L5	1.35	1.75	2.10	2.73	1.59	2.66	1.94
L7	2.57	3.33	3.75	4.87	1.65	2.76	2.03
L9	0.30	0.40	0.78	1.01	0.50	0.84	0.70
L10	1.62	2.11	2.48	3.23	2.06	3.44	2.58
L12	0.94	1.22	1.50	1.95	1.20	2.01	1.55
U2	0.69	0.89	1.02	1.33	0.90	1.50	1.06
U4	1.85	2.40	2.81	3.65	2.19	3.66	2.67
U6	1.19	1.54	1.95	2.54	1.76	2.94	2.09
U8	1.10	1.42	1.84	2.39	1.65	2.76	2.03
U10	3.66	4.74	5.24	6.81	3.22	5.38	3.94
U11	0.59	0.76	1.08	1.41	0.86	1.43	1.12
U13	1.72	2.23	2.61	3.40	1.93	3.22	2.42

Table 6-5 Rating Factors for BR 101-217 Joints Using the TEP

	MBE - LRFR Strength I		MBE - LRFR Service II		MBE - LFR		BDM - LRFR
Joint ID	Inventory	Operating	Inventory	Operating	Inventory	Operating	
L1	1.16	1.51	1.83	2.38	1.33	2.22	1.69
L2	1.46	1.89	2.25	2.92	1.75	2.91	2.08
L3*	0.48	0.62	0.98	1.27	0.67	1.12	0.89
L5*	0.86	1.12	1.50	1.95	1.08	1.81	1.37
L6	1.08	1.40	1.74	2.27	1.28	2.14	1.61
L7	0.73	0.95	1.25	1.63	0.89	1.49	1.15
L8	0.84	1.09	1.31	1.71	0.94	1.57	1.21
L9	0.79	1.02	1.24	1.61	0.87	1.45	1.15
L11	1.30	1.30	2.40	3.13	1.71	2.85	2.24
U2#	0.50	0.65	0.93	1.21	0.66	1.10	0.85
U3#	0.58	0.75	1.07	1.40	0.76	1.27	0.98
U4	1.12	1.45	1.92	2.49	1.43	2.39	1.76
U5	1.02	1.32	1.68	2.19	1.22	2.04	1.55
U6	1.40	1.81	2.14	2.79	1.58	2.64	1.98
U7	0.92	1.19	1.50	1.95	1.08	1.81	1.38
U9	0.72	0.93	1.15	1.49	0.81	1.36	1.06
U10	1.12	1.46	1.69	2.20	1.20	2.01	1.57

* Indicates joints where all RFs would be greater 1.0 if compressions chords that are milled-to-bear were neglected. # Indicates joints where all RFs would be greater than 1.0 if chords were neglected due to the splice being well outside the interference zone.

Of the joints with RFs less than 1.0 several of them have configurations that would likely result in the assignment of an RF greater than 1.0 after a closer look. For example, several joints are marked as having compression chords that are specified as “milled-to-bear” on the drawings as the example shown in Figure 6-1 demonstrates. For those joints indicated, if the compression chords were omitted from the TEP since they are not transferring stress into the gusset plate, the RFs would be greater 1.0. A second joint configuration that may result in overly conservative rating factors when the TEP is applied is the case of chord splices well outside the interference zone, such as that shown in Figure 6-2. In this case, the assumption of interfering stresses made in

the derivation of the TEP yield check is likely overly conservative since the splice is removed from where the stresses from the diagonal or vertical would be expected to interact. Joints with these conditions are indicated in Tables Table 6-3 through 6-5. If these joints are considered to have a RF greater than 1.0, which would be the case given the discussion above, then no joints are identified as likely to be yielding under in the MBE LRFR method under the Service II load combination at the inventory load level.

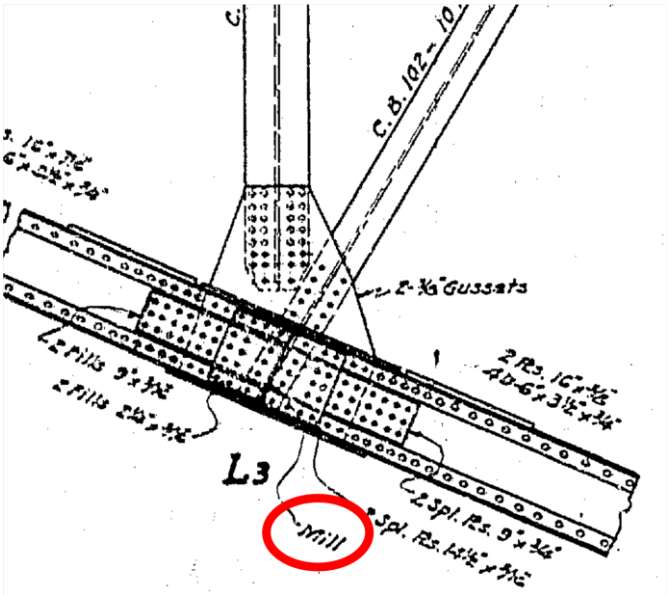

Figure 6-1 Example of Joint with Milled-to-Bear Compression Chords from BR 101-217.

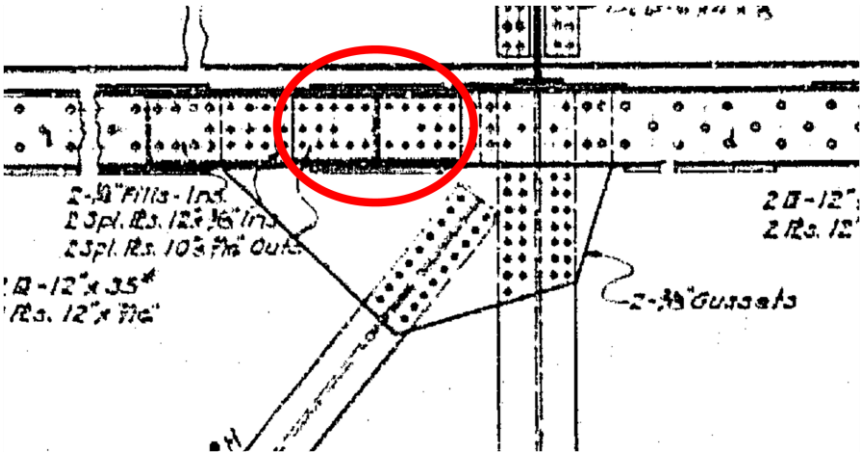

Figure 6-2 Example of Joint with Chords Spliced Outside Interference Zone from BR 101-

6.3.2 Comparison with FHWA Load Ratings

The RFs computed using the FHWA Guide procedure were computed using the MBE LRFR method for the Strength I load combination at the inventory load level and were compared to the RFs from the TEP using the Service II load combination at the inventory load level. Tables 6-6 through 6-8 compare the RFs for the two cases and demonstrate that the TEP applied at service loads is consistently conservative relative to the FHWA Guide procedure applied at strength loads. For BR 101-217 where the vertical or diagonal member pass through the work point to the top or bottom of the gusset, as shown in 6-1 and 6-2, it was not possible to draw unobstructed lines for the vertical and horizontal shear checks in the FHWA Guide. Therefore, the shear checks were not included in those cases. The tables also show the governing limit state from the FHWA Guide procedure. The Strength I load combination for the FHWA Guide procedure and the Service II load combination for the TEP were selected because the FHWA Guide methods focus on failure modes while the TEP is focused on the onset of yielding. If it is demonstrated that the TEP is conservative relative to the FHWA Guide procedures using these load combinations it is also ensured to be conservative when used with the Strength I load combination as those loads are larger than the Service II loads.

Table 6-6 Rating factors for BR 90-134N Joint from the TEP with Service II Loads at Inventory Level and the FHWA Guide with Strength I Loads at Inventory Level

	Joint Identification			
	U1	U3	L2	L4
Triage RF	2.33	1.41	2.20	2.00
FHWA RF	3.51	4.09	2.59	2.75
FHWA Mode[1]	HS	VS	C	GSY

[1]GSY = Gross Section Yielding, HS = Horizontal Shear, VS = Vertical Shear, BS = Block Shear, C = Compression Buckling

Table 6-7 Rating factors for BR 31-36 Joints from the TEP with Service II Loads at Inventory Level and the FHWA Guide with Strength I Loads at Inventory Level

	Joint Identification						
	U2	U4	U6	U8	U10	U11	U13
Triage RF	1.02	2.81	1.95	1.84	5.24	1.08	2.61
FHWA RF	1.24	2.83	2.19	1.90	5.44	1.49	4.85
FHWA Mode[1]	HS	VS	HS	HS	VS	VS	C
	Joint Identification						
	L1	L3	L5	L7	L9	L10	L12
Triage RF	1.13	1.82	2.10	3.75	0.78	2.48	1.50
FHWA RF	1.23	1.96	2.12	5.32	0.95	3.14	1.95
FHWA Mode[1]	HS	VS	HS	C	HS	VS	HS

[1]GSY = Gross Section Yielding, HS = Horizontal Shear, VS = Vertical Shear, BS = Block Shear, C = Compression Buckling

Table 6-8 Rating factors for BR 101-217 Joints from the TEP with Service II Loads at Inventory Level and the FHWA Guide with Strength I Loads at Inventory Level

	Joint Identification							
	U2	U3	U4	U5	U6	U7	U9	U10
Triage RF	0.93	1.07	1.92	1.68	2.14	1.50	1.15	2.38
FHWA RF	1.35	1.55	2.47	2.29	2.79	2.02	2.86	2.94
FHWA Mode[1]	GSY	GSY	BS	GSY	GSY	BS	GSY	GSY

	Joint Identification								
	L1	L2	L3	L5	L6	L7	L8	L9	L11
Triage RF	1.83	2.25	0.98	1.50	1.74	1.25	1.31	1.24	2.40
FHWA RF	1.84	2.56	1.78	2.47	2.34	2.79	2.53	2.25	3.39
FHWA Mode[1]	C	C	C	GSY	GSY	GSY	GSY	GSY	BS

[1]GSY = Gross Section Yielding, HS = Horizontal Shear, VS = Vertical Shear, BS = Block Shear, C = Compression Buckling

The tables above indicate that the single joint of the three bridges considered that has an RF of less than 1.0 using the FHWA Guide procedures, Joint L9 from BR 31-36, also has an RF of less than 1.0 from the TEP. Additionally, if the RFs less than 1.0 from the TEP for bridge 101-217 are not considered as they are resulting from compression chords that are milled-to-bear and tension chords with splices outside the interference zone, only Joint L9 has an RF of less than 1.0 from the TEP. Thus, using the TEP at service loads is both conservative relative to the FHWA Guide approach and is also consistent with the FHWA Guide approach in identifying the same joint as having insufficient capacity at the inventory load levels. It should be noted that the TEP would be consistently conservative relative to the FHWA Guide approach for all other rating methods described in the previous section. Further, the TEP may employed at with strength load combinations but will generate conservative results. Joints found to RFs less than 1.0 with the TEP applied at strength load combinations could then be evaluated with the TEP and service loads to determine whether any additional action might be warranted.

6.3.3 Load Ratings Including Rivets

As discussed, the RFs above do not include rivet shear as a possible limit state so that the gusset plate checks in the TEP and FHWA Guide could be compared. The FHWA Guide recommends rivet shear strengths as given in Table 6-9, which depend on the age of the bridge. Given the ages of the bridges considered here, the rivets for BR 90-134N and BR 31-36 would be assigned a shear strength of 145 MPa (21 ksi) and the rivets of BR 101-217 would be assigned a shear strength of 124 MPa (18 ksi). RFs were calculated for the joints of the three bridges using these shear strengths and only the rivet limit state. The resulting RFs are shown in Tables 6-10 through Table 6-12 for the MBE LRFR rating method and the MBE LFR method. As shown almost all the RFs found only from the rivet shear strength are smaller than RFs for the gusset plate limit states. Further, many of the RFs are less than 1.0, with only one joint having an RF greater 1.0 for the MBE LRFR rating method at the Strength I limit state and inventory load level and only three joints have RFs greater 1.0 for the MBE LFR rating method at the inventory load levels. BR 101-217 has many RFs less than 1.0 for all rating methods and load levels. These results indicate that either many of the rivets on these bridges need replacement or that the recommended rivet strengths are too low.

Table 6-9 Rivet Shear Strengths as Given by the FHWA Guide

Year of Construction	ϕF MPa (ksi)
Constructed prior to 1936 or of unknown origin	124 (18)

Constructed after 1936 but of unknown origin	145 (21)
ASTM A 502 Grade I	186 (27)
ASTM A 502 Grade II	220 (32)

Table 6-10 Rating Factors Considering only Rivet Strength for BR 90-134N Joints

	MBE - LRFR Strength I		MBE - LRFR Service II		MBE - LFR	
Joint ID	Inventory	Operating	Inventory	Operating	Inventory	Operating
L2	0.67	0.87	1.23	1.59	0.86	1.44
L4	1.02	1.33	1.78	2.31	1.27	2.12
U1	0.67	0.87	1.23	1.59	0.79	1.31
U2	0.60	0.78	1.22	1.59	0.85	1.41

Table 6-11 Rating Factors Considering only Rivet Strength for BR 31-36 Joints

	MBE - LRFR Strength I		MBE - LRFR Service II		MBE - LFR	
Joint ID	Inventory	Operating	Inventory	Operating	Inventory	Operating
L1	0.90	1.17	1.35	1.76	0.93	1.55
L3	0.92	1.20	1.38	1.80	0.95	1.59
L5	0.74	0.96	1.31	1.70	0.94	1.57
L7	0.66	0.86	1.25	1.62	0.89	1.49
L9	0.72	0.93	1.31	1.70	0.93	1.55
L10	0.66	0.85	1.18	1.53	0.82	1.37
L12	0.87	1.13	1.39	1.81	0.96	1.60
U2	0.61	0.79	0.91	1.18	0.71	1.19
U4	0.82	1.06	1.42	1.84	1.07	1.79
U6	0.66	0.86	1.25	1.62	0.93	1.55
U8	0.66	0.86	1.25	1.63	0.89	1.49
U10	0.64	0.83	1.16	1.51	0.75	1.25
U11	0.74	0.95	1.28	1.67	0.90	1.51
U13	0.99	1.28	1.52	1.98	1.10	1.83

Table 6-12 Rating Factors Considering only Rivet Strength for BR 101-217 Joints

	MBE - LRFR Strength I		MBE - LRFR Service II		MBE - LFR	
Joint ID	Inventory	Operating	Inventory	Operating	Inventory	Operating
L1	0.65	0.84	1.00	1.30	0.68	1.13
L2	0.53	0.69	1.00	1.30	0.72	1.20
L3	0.51	0.67	1.01	1.31	0.72	1.21
L5	0.40	0.52	0.85	1.10	0.58	0.96
L6	0.39	0.50	0.81	1.06	0.55	0.92
L7	0.65	0.85	1.14	1.48	0.81	1.34
L8	0.61	0.79	1.05	1.36	0.73	1.22
L9	0.37	0.48	0.68	0.88	0.45	0.75
L11	0.67	0.87	1.03	1.34	0.70	1.16
U2	0.64	0.82	1.09	1.41	0.79	1.32
U3	0.43	0.56	0.88	1.14	0.60	1.01
U4	0.40	0.52	0.85	1.10	0.58	0.96
U5	0.33	0.43	0.75	0.98	0.49	0.82
U6	0.58	0.75	1.07	1.39	0.75	1.25
U7	0.55	0.71	0.85	1.10	0.61	1.02
U9	0.58	0.75	0.96	1.25	0.67	1.12
U10	0.54	0.70	0.91	1.18	0.62	1.04

Section 7 Historical Evaluation of Rivet Strength

7.1 Historical Rivet Testing Programs

A preliminary investigation of the rivet shear strength recommended in the FHWA Guide including a survey of literature on the testing of riveted joints was conducted. Data was gathered from experiments conducted from 1904-1941 on a variety of riveted joints having various configurations, rivet materials and plate materials. The experimental programs are briefly summarized below followed by a discussion of their results.

The American Railway Engineering and Maintenance-of-Way Association (AREMA) conducted tests on various joint configurations, from single rivet joints to joints with multiple rivets and layered splice plates (AREMA 1904), for a total of 90 individual tests. Both the rivet and plate material was specified as Open-Hearth (OH) steel. Force-displacement plots were recorded for all joints and rivet shear stresses for each joint were calculated assuming an even distribution of load to each rivet. Connections were tested to failure of either the rivets or the plates.

Talbot and Moore (1911) tested joints that were modeled after the AREMA (1904) tests but had different rivet materials. They conducted 90 tests on joints with rivets made with nickel-steel and 54 tests on joints with chrome-nickel steel. Total force and connection deformation were recorded and the loads were assumed to be evenly distributed to the rivets for calculating the individual rivet stress. Connections were again tested to failure.

Davis et al. (1939) tested 37 different joint configurations where the number of rivets and number of splice plates were varied between specimens. The rivet and plate materials were also varied with both carbon-steel and manganese-steel rivets investigated. Davis et al. introduced the concept of effective rivet yield (ERY) discussed below and outlined the general behavior of rivets through failure. All connections were tested to failure and the load was again assumed to be evenly distributed to each rivet.

Wilson et al. (1941) tested 63 joints in seven different joint configurations. Three different low alloy steels (denoted A, B and C) were used for the rivets. Munse and Cox (1956) tested individual rivets without driving them into holes in a setup that could subject the rivets to varying degrees of combined tension and shear. The rivet diameter and grip length were also varied. From this extensive testing program data on 44 rivets loaded only in shear was obtained.

7.2 Effective Rivet Yield

The concept of ERY was introduced by Davis et al. (1939) as a method for describing the rivet yield point of riveted connection. Figure 7-1 shows typical rivet shear stress versus joint set behavior for a riveted joint under axial load which has been divided into four different stages. Joint set is defined as a permanent deformation of the joint and includes the mechanisms of slip, bearing and rivet deformation. In the tests described in the literature, these curves are usually given for the entire joint where the rivet shear stress has been calculated assuming a uniform distribution of load to each rivet.

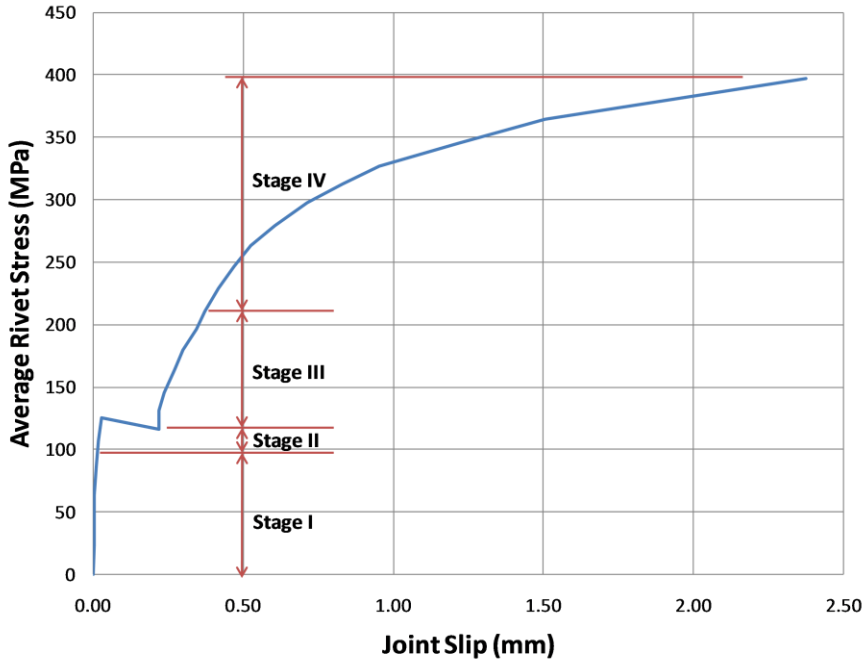

Figure 7-1 General Rivet Shear Stress vs. Joint Slip Behavior.

Stage I of the joint behavior is prior to slip of the rivets where the load is transferred from one plate to the other via friction. The end of this stage depends on the number of rivets in the connection and is generally taken as the point when the load is sufficient to cause movement of the joint as a whole, i.e., when the slip begins at the middle of the joint. Stage II is the region of behavior where slip at any section of a joint increases at a greater rate than the load. The slope of the shear stress versus joint deformation in Stage II is dependent on the number of rivets in the joint, the grip length of the rivets and corresponding rivet clamping force, and whether the connections are in single or double shear. Stage II is generally very short, with joint set values typically less than $1/100^{th}$ of an inch even in connections with relatively few rivets. As the

number of rivets increases the stiffness of the connection in Stage II will also increase. Stage III is the region of behavior where the rivets are transferring load largely through bearing which generally results in a large increase in the joint stiffness and is again dependent on the connection configuration. Stage IV begins when yielding occurs in plates, rivets, or both and joint set again increases more rapidly with load. For "over-riveted joints" yielding occurs in plates and for "under-riveted joints" yielding occurs in rivets. The transition from Stage III to Stage IV is defined as the ERY and occurs when the stiffness of the joint is ½ of the initial Stage III stiffness. Following ERY, the connections reach a peak capacity where either the rivets fracture or the connected plates fracture.

7.3 Collected Rivet Connection Data

Table 7-1 shows the collected data from the testing programs described above. The table included information on the rivet steel's basic tensile properties including yield and tensile strengths, the number of joints tests where data was used to compute ERY and the resulting statistics for ERY, and the number of joints where data on ultimate rivet shear strength was collected and the resulting statistics. Note that only joints where rivet fracture was the governing failure mode were included in the latter, thus the number of tests used for computing ERY and ultimate rivet shear stress, V_u, are not the same. Further, ERY is not reported for the tests by Munse and Cox (1956) because they did not give full shear stress or force versus joint set results and only reported ultimate rivet strengths. ERY was computed for each test by digitizing the rivet shear stress versus joint set curves using scanned figures and a software program capable of converting pixel data for a xy plot to numerical data.

Comparing the collected data shown in Table 7-1 with the recommended FHWA values, which for convenience are repeated at the bottom of Table 7-1, demonstrates that the strength recommended by FHWA may be overly conservative. It seems that the recommended strengths align better with ERY than with the ultimate strengths of riveted joints. It should be noted that this analysis does not consider two important items: (i) the strength of existing rivets after years in service and the effects of the corrosion that may be present, and (ii) the calibration of the resistance factor, ϕ, that is included in the FHWA values. However, the FHWA values are recommended for use in checking connections at the Strength I load combination where ultimate strengths and failure modes are typically used as limit states. From the data presented here, it appears that the recommended values may be overly conservative for that application. Additional rivet testing is necessary to make recommendations regarding the rivet strengths that should be

used for load rating joints with a particular focus on correlating the age of the rivets to the FHWA recommendations and historical data and investigating the impact of corrosion.

Table 7-1 Rivet Shear Strengths Data Collected from the Literature

Reference	Steel Material Type	Rivet Tensile Properties		ERY Data MPa (ksi)			Ultimate Shear Strength Data MPa (ksi)		
		F_y MPa (ksi)	F_u MPa (Ksi)	No. of Tests	Mean	Std. Dev.	No. of Tests	Mean	Std. Dev.
AREMA (1904)	OH Steel	244.0 (35.4)	415.7 (60.3)	80	159.9 (23.2)	23.4 (3.4)	33	334.4 (48.5)	19.3 (2.8)
Talbot and Moore (1911)	Nickel Steel	310.2 (45)	472.2 (68.5)	90	192.3 (27.9)	23.4 (3.4)	90	390.2 (56.6)	12.4 (1.8)
	Chrome-Nickel Steel	264.7 (38.4)	406.7 (59.0)	54	205.4 (29.8)	20.0 (2.9)	54	364.0 (52.8)	17.2 (2.5)
Woodruff and Davis (1939)	Carbon Steel	274.4 (39.8)	397.1 (57.6)	5	226.1 (32.8)	10.3 (1.5)	5	366.8 (53.2)	17.2 (2.5)
	Manganese Steel	376.4 (54.6)	558.4 (81.0)	9	319.2 (46.3)	15.9 (2.3)	9	517.7 (75.1)	17.2 (2.5)
Wilson et al. (1940)	Low Alloy Steel "A"	361.2 (52.4)	510.8 (74.1)	21	264.0 (38.3)	37.9 (5.5)	6	432.3 (62.7)	13.8 (2.0)
	Low Alloy Steel "B"	295.8 (42.9)	452.2 (65.6)	21	260.6 (37.8)	27.6 (4.0)	3	446.7 (64.8)	4.1 (0.8)
	Low Alloy Steel "C"	338.5 (49.1)	526.0 (76.3)	21	298.5 (43.3)	30.3 (4.4)	6	504.0 (73.1)	26.2 (3.8)
Munse and Cox (1956)	ASTM A 141	193.1 (28.0)	358.5 (52.0)	-	-	-	44	363.3 (52.7)	32.4 (4.7)
FHWA: Constructed prior to 1936 or of unknown origin								124 (18)	
FHWA: Constructed after 1936 but of unknown origin								145 (21)	
FHWA: ASTM A 502 Grade I								186 (27)	
FHWA: ASTM A 502 Grade II								220 (32)	

7.4 Rivet RF's Using ERY and Revised Ultimate Shear Strengths

Recently there has been discussion about the recommended rivet shear strengths given in the FHWA Guide. It is clear that these values are conservative with respect to the data given in the test programs reviewed in this Chapter. In light of the fact that almost every joint would need to have some, if not all, of the rivets replaced if the current strength recommendations are used, internal discussions at the FHWA have proposed using revised rivet strengths, as shown in Table 7-2 (C.W. Roeder, personal communication, December 5, 2010). Using these revised strengths, RF's were calculated, considering only the rivets, using the MBE LRFR Strength I and Service II limit states at both the Inventory and Operating load levels. These results are shown in Table 7-3 through Table 7-5.

Looking at these results it is clear that using these revised rivet strengths dramatically decreases the number of joints with RF less than 1.0. In fact, only two joints have RF less than 1.0 using the MBE LRFR Strength I limit state at Inventory load levels.

Table 7-2 Proposed FHWA Guide rivet strength revisions

Rivet Type	ϕF (ksi)
Rivets of unknown origin	27
Documentable C content > 0.18% or ASTM A 502 Grade I	33
ASTM A 502 Grade II	43

Table 7-3 Rating Factors considering only revised rivet strengths for BR 90-134N Joints

	MBE - LRFR Strength I		MBE - LRFR Service II	
Joint ID	Inventory	Operating	Inventory	Operating
L2	1.17	1.52	1.90	2.47
L4	1.70	2.21	2.69	3.50
U1	1.17	1.52	1.88	2.45
U2	1.17	1.52	1.86	2.42

Table 7-4 Rating Factors considering only revised rivet strengths for BR 31-36 Joints

	MBE - LRFR Strength I		MBE - LRFR Service II	
Joint ID	Inventory	Operating	Inventory	Operating
L1	1.29	1.68	1.88	2.45
L3	1.32	1.71	1.91	2.48
L5	1.25	1.63	1.90	2.47
L7	1.19	1.55	1.96	2.55
L9	1.25	1.62	203	2.63
L10	1.13	1.46	1.81	2.36
L12	1.33	1.72	1.92	2.50
U2	0.87	1.13	1.27	1.65
U4	1.36	1.76	2.14	2.79
U6	1.19	1.55	1.96	2.55
U8	1.20	1.56	1.98	2.57
U10	1.12	1.45	1.81	2.36
U11	1.23	1.59	1.95	2.54
U13	1.45	1.88	2.06	2.68

As mentioned previously, a conservative estimate of the ultimate shear strength of a rivet is given by $\sigma_u = 0.75F_u$. In the case where a bridge has a number of joints with rivet RF's less than 1.0, it might be advantageous for the bridge owner to remove a number of rivets from the bridge and perform tests to determine their ultimate tensile strength, F_u. Using this value the ultimate rivet shear strength could be determined and then used to recalculate the rivet RF's. Using this notion, RF's for the three WSDOT bridges were calculated using ultimate rivet strengths calculated from rivet tensile strength data from test programs of a similar age. Table 7-6 shows the ultimate rivet strength used to calculate the rivet RF's using the MBE LRFR Strength I limit state under Inventory and Operating load levels. In this case φ was assumed to be 0.75. The rivet RF's calculated using these values are shown in

Table 7-7 through Table 7-9. Examining these results, only one joint has a RF less than 1.0 under the Inventory load level using this method of determining ultimate rivet strengths.

Table 7-5 Rating Factors considering only revised rivet strengths for BR 101-217 Joints

	MBE - LRFR Strength I		MBE - LRFR Service II	
Joint ID	Inventory	Operating	Inventory	Operating
L1	1.19	1.55	1.74	2.26
L2	1.29	1.67	2.02	2.63
L3	1.31	1.70	2.08	2.71
L5	1.13	1.46	1.83	2.37
L6	1.08	1.39	1.74	2.26
L7	1.42	1.84	2.18	2.83
L8	1.30	1.68	1.97	2.56
L9	0.86	1.11	1.34	1.74
L11	1.22	1.58	1.77	2.30
U2	1.34	1.74	2.04	2.65
U3	1.15	1.49	1.85	2.40
U4	1.13	1.46	1.83	2.37
U5	1.01	1.32	1.67	2.18
U6	1.36	1.77	2.13	2.77
U7	1.01	1.31	1.46	1.90
U9	1.18	1.53	1.77	2.30
U10	1.12	1.45	1.69	2.19

Table 7-6 Rivet ultimate shear strength calculated for the three WSDOT bridges using rivet test program data of a similar age

Bridge ID	Year Constructed	Rivet Test Program of a Similar Age	Rivet Material Tensile Strength, F_u (ksi)	φF_n (ksi)
BR 90-134N	1949	Munse et al. (1956)	52	29
BR 31-36	1950	Munse et al. (1956)	52	29
BR 101-217	1930	Woodruff et al. (1939)	58	32

Table 7-7 Rating Factors considering only rivet strengths based on F_u for BR 90-134N Joints

	MBE - LRFR Strength I	
Joint ID	Inventory	Operating
L2	1.34	1.74
L4	1.93	2.50
U1	1.34	1.74
U2	1.36	1.76

Table 7-8 Rating Factors considering only rivet strengths based on F_u for BR 31-36 Joints

	MBE - LRFR Strength I	
Joint ID	Inventory	Operating
L1	1.42	1.85
L3	1.45	1.88
L5	1.43	1.85
L7	1.37	1.78
L9	1.43	1.85
L10	1.29	1.67
L12	1.46	1.89
U2	0.96	1.24
U4	1.54	1.99
U6	1.37	1.78
U8	1.38	1.79
U10	1.27	1.65
U11	1.39	1.81
U13	1.59	2.06

Table 7-9 Rating Factors considering only rivet strengths based on F_u for BR 101-217 Joints

	MBE - LRFR Strength I	
Joint ID	Inventory	Operating
L1	1.50	1.94
L2	1.70	2.21
L3	1.75	2.27
L5	1.53	1.98
L6	1.46	1.89
L7	1.85	2.40
L8	1.68	2.18
L9	1.13	1.47
L11	1.53	1.98
U2	1.73	2.25
U3	1.55	2.01
U4	1.53	1.98
U5	1.40	1.81
U6	1.80	2.33
U7	1.26	1.64
U9	1.51	1.96
U10	1.44	1.87

In a similar fashion, ERY strength values could be determined by the bridge owner using material properties of rivets. Looking at the values in Table 7-1, an appropriate method for determining ERY as a function of the rivet material yield strength, F_y, is given by:

$$\text{For bridges constructed prior 1930} \quad ERY = 0.5F_y \tag{1.1.1}$$

$$\text{For bridges constructed after 1930} \quad ERY = 0.7F_y \tag{1.1.2}$$

The rivet material yield strengths were taken from the same test programs shown in Table 7-1 and then ERY strengths were calculated, as shown in Table 7-10. Using these ERY strengths, rivet RF's for the three WSDOT bridges were calculated using the MBE LRFR Service II limit state under Inventory and Operating load levels and are shown in Table 7-11 through Table 7-13. It

should be noted that the value used for φ was 0.90; a value typically used for the yield strength of ductile materials.

Looking at these results, 21 of the joints have RF's less than 1.0 under the Inventory load level compared to only three at Operating load levels. Using ERY strength results in more RF's less than 1.0 than if the results shown in the FHWA Guide are used.

Table 7-10 ERY values calculated for the three WSDOT bridges using rivet test program data of a similar age

Bridge ID	Year Constructed	Rivet Test Program of a Similar Age	Rivet Material Tensile Yield Strength, F_y (ksi)	φERY (ksi)
BR 90-134N	1949	Munse et al. (1956)	28	18
BR 31-36	1950	Munse et al. (1956)	28	18
BR 101-217	1930	Woodruff et al. (1939)	40	18

Table 7-11 Rating factors considering only rivet strengths based on ERY for BR 90-134N Joints

	MBE - LRFR Service II	
Joint ID	Inventory	Operating
L2	0.89	1.15
L4	1.32	1.72
U1	0.89	1.15
U2	0.84	1.09

Table 7-12 Rating Factors considering only rivet strengths based on ERY for BR 90-134N Joints

	MBE - LRFR Service II	
Joint ID	Inventory	Operating
L1	1.09	1.41
L3	1.12	1.45
L5	0.96	1.25
L7	0.89	1.16
L9	0.95	1.23
L10	0.86	1.12
L12	1.11	1.45
U2	0.73	0.95
U4	1.05	1.37
U6	0.89	1.16
U8	0.89	1.16
U10	0.84	1.10
U11	0.95	1.24
U13	1.24	1.62

Table 7-13 Rating Factors considering only rivet strengths based on ERY for BR 101-217 Joints

	MBE - LRFR Service II	
Joint ID	Inventory	Operating
L1	1.00	1.30
L2	1.00	1.30
L3	1.01	1.31
L5	0.85	1.10
L6	0.81	1.06
L7	1.14	1.48
L8	1.05	1.36
L9	0.68	0.88
L11	1.03	1.34
U2	1.09	1.41
U3	0.88	1.14
U4	0.85	1.10
U5	0.75	0.98
U6	1.07	1.39
U7	0.85	1.10
U9	0.96	1.25
U10	0.91	1.18

Section 8 Conclusions and Recommendations

8.1 Conclusions

The currently recommended FHWA procedures for gusset plate evaluation may not identify all gusset plates in steel truss bridges that may be yielding under service loads. Analysis results indicate that a complex interaction of stresses is generated in gusset plates by connecting members and that this interaction can initiate gusset plate yielding when the uniaxial stresses on Whitmore sections associated with those connecting members are well below yield. Simple mechanics were used to develop a conservative and considerably simpler process for identifying gusset plates that may be yielding of buckling. Gusset plates failing this triage evaluation

procedure may still be adequate, but require more detailed evaluation. Detailed finite element analysis indicated this method conservatively predicted the onset of gusset plate yielding and was consistently conservative relative to the procedures in the FHWA Guide, but it is quicker and easier than the FHWA method. This is the yield check of the recommended Triage Evaluation Procedure (TEP) for which an automated spreadsheet has been developed and is described in the Appendix.

Gusset plate buckling did not occur prior to gusset plate yielding in any of the connections studied at their actual gusset plate thicknesses. When buckling may be a concern, the Modified Thornton Method of evaluating the gusset plate unbraced length and compressive stress, along with an effective length factor of 1.0, was found to be conservative when used with the AASHTO buckling equations. This method is included as the buckling check in the TEP and automated spreadsheet.

When applied to three bridges in Washington State, the proposed TEP was found to be simple and appropriately conservative. It resulted in rating factors (RFs) that were conservative relative to those values in the FHWA Guide and when applied at service loads or operating load levels very few joints were identified as needing further investigation (i.e., having an RF less than 1.0).

When the rivet strengths recommended in the FHWA Guide were employed to calculate RFs, it was shown that many joints of the three bridges considered had RFs less than 1.0. Comparison of the recommended rivet strengths with strengths obtained from experimental results in the literature indicate that the recommended values may be overly conservative, although additional research is necessary including experiments on rivets after years of service.

8.2 Recommendations

The TEP and automated spreadsheet are recommended for load rating joints in truss bridges for the limit states of the onset of gusset plate yielding and gusset plate compressive buckling. Rivet shear strength should also be evaluated and until additional research is completed the values recommended in the FHWA Guide seem to provide a very conservative lower bound.

8.3 Recommendations for Future Research

The assessment of rivet strength in older steel truss bridges and a comparison with historical data on the strength of like new rivets is a critical area for future research. As shown here, the rating factors for a majority of joints on the three truss bridges studied were less than 1.0 and controlled

by the rivet strength when current strength recommendations from the FHWA Guide were used. A brief literature review demonstrated that the current recommendations are very conservative relative to historical tests data. However, that historical data is based on tests of pristine connections built in laboratory conditions. Those strengths may be different than those found from testing joints in existing bridges. Thus, it is recommended that a study of the strength of rivets from existing construction be conducted to develop appropriate recommendations.

The impact of layered splice plates on the transfer and distribution of stress in gusset plates is not understood and should be investigated. Such layered connections were outside the scope of this project but there are many examples of such connections in the bridge inventory. Current practice with the use of the procedures in the FHWA Guide is to simply add the area of the plates together when they overlap in regions being evaluated for the shear check and Whitmore check. However, this assumes that the stresses in the plates are equal, which may not be the case. Further, the impact of the layered gusset plates on buckling is not well understood. Currently the plates are treated as a fully composite member, which may overestimate the buckling strength if instead the act as completely separate members.

Section 9 References

AASHTO (2007). *LRFD Bridge Design Specifications*, American Association of State Highway and Transportation Officials.

AASHTO (2008), *Manual for Bridge Evaluation, 1st Edition*, American Association of State Highway and Transportation Officials.

AISC (2002), *Specifications for Structural Steel Buildings*, American Institute of Steel Construction.

Astaneh-Asl, A, (1989) "Simple Methods for Design of Gusset Plates," Proceedings ASCE Structures Conference, San Francisco, CA, p345-354

ANSYS (2008), *ANSYS Release 11 Reference Manual*, ANSYS, Inc.

AREMA (1904). "Tests of Riveted Joints*",* American Railway Engineering and Maintenance-of-Way Association, *Proceedings*, Vol. 6, p272-484.

ASTM (1924). *ASTM A7 Standard Specifications for Structural Steel for Bridges*. American Society for Testing and Materials.

ASTM (1939). *ASTM A7-39 Standard Specifications for Structural Steel for Buildings and Bridges*. American Society for Testing and Materials.

ASTM (1946). *ASMT A94-46 Standard Specifications for Structural Silicon Steel*. American Society for Testing and Materials.

Bjorhovde, R., and Chakrabarti, S. K., (1985) "Test of Full Size Gusset Plate Connections", ASCE, *Journal of Structural Engineering*, Vol. 111, No. 3, p667- 684.

Brockenbrough, R.L., (2002) *Design Guide 15: AISC Rehabilitation and Retrofit Guide*, American Institute of Steel Construction.

Brown, V. L. S., (1998) "Stability of Gusseted Connections in Steel Structures", Doctoral Dissertation, University of Delaware

CSI (2008). *SAP2000 Linear and Nonlinear Static and Dynamic Analysis and Design of Three-Dimensional Structures, Reference Manual*, Computers and Structures, Inc.

Davis, R.E., Woodruff, G.B., and Davis, H.E., (1939) "Tension Tests of Large Riveted Joints", ASCE, *Transaction of the American Society of Civil Engineers*, Vol. 105, No. 2084, p1193-1299.

FHWA (2009). *Load Rating Guidance and Examples for Bolted and Riveted Gusset Plates in Truss Bridges.* Publication No. FHWA-IF-09-014, Federal Highway Administration.

Hardash, S.G. and Bjorhovde, R., (1985) "New Design Criteria for Gusset Plate in Tension", AISC, *Engineering Journal*, Vol. 22, No. 2, p77-94

Higgins, C., Senturk, A.E., and Turan, O.T. (2010). "Comparison of Block Shear and Whitmore Section Methods for Load Rating Existing Steel Truss Gusset Plate Connections", *Journal of Bridge Engineering*, Vol 15, No. 2, p160-171.

Munse, W.H., and Cox, H.L. (1956) “The Static Strength of Rivets Subjected to Combined Tension and Shear”, University of Illinois, *Bulletins of the Engineering Experiment Station*, No. 437.

NTSB (2008), “Structural Investigation Group Chairman Factual Report, Report No. 08-115,” National Transportation Safety Board, Washington D.C., March 5, 2008.

Ocel, J.M. and Wright, W.J. (2008). *Finite Element Modeling of I-35 Bridge Collapse, Final Report*, Turner-Fairbank Highway Research Center Report, Federal Highway Administration.

Olson, A.W. (2010). “Triage Evaluation of Gusset Plates in Steel Truss Bridges”, MSCE Thesis, University of Washington.

Roeder, C.W., Lehman, D.E., and Yoo, J.H., (2005) "Improved Seismic Design of Steel Frame Connections," *International Journal of Steel Structures*, Korean Society of Steel Construction, Seoul, Korea, Vol. 5, No. 2, pgs 141-53.

Sheng, N., Yam, M. C. H., and Lu, V.P., (2002) “Analytical Investigation and the Design of the Compressive Strength of Steel Gusset Plate Connections”, Journal of Constructional Steel Research, v 58, p 1473-1493

Talbot, A.N. and Moore, H.F. (1911) “Tests of Nickel-Steel Riveted Joints”, University of Illinois, *Bulletins of the Engineering Experiment Station*, Vol. 7, No. 49, p1-53.

Thornton, W.A., (1984) “Bracing Connections for Heavy Construction”, AISC, *Engineering Journal*, Vol. 21, No 3, p139-148

WSDOT (2010). *Bridge Design Manual LRFD*, Washington State Department of Transportation.

Whitmore, R.E., (1952) “Experimental Investigation of Stresses in Gusset Plates”, Bulletin NO. 16, Engineering experiment station, University of Tennessee.

Wilson, W.M., Bruckner, W.H., and McCrackin, T.H., (1942) “Tests of Riveted and Welded Joints in Low-Alloy Structural Steels”, University of Illinois, *Bulletins of the Engineering Experiment Station*, No. 337.

Yam, M.C.H. (1994). “Compressive Behavior and Strength of Steel Gusset Plate Connections.” Doctoral Dissertation, University of Alberta.

Yam, M. C. H, and Cheng, J. J. R., (2002) “Behavior and Design of Gusset Plate Connections in Compression”, *Journal of Constructional Steel Research*, v 58, n 5-8, p 1143-1159

Yoo, J.H. (2006). “Analytical Investigation on the Seismic Performance of Special Concentrically Braced Frames”, Ph.D. Dissertation, University of Washington.

Yoo, J.H., Roeder, C.W., and Lehman, D.E., (2008) "FEM Simulation and Failure Analysis of Special Concentrically Braced Frame Tests," ASCE, *Journal of Structural Engineering*, Vol.134, No. 6, Reston, VA, pgs 881-89.

Appendix AThe TEP Spreadsheet

This section contains a description of and instructions for using the TEP spreadsheet that has been provided to WSDOT. For each joint a careful assessment of the geometry is necessary as this is the key input for the spreadsheet.

The first step in using the TEP spreadsheet is the input of the basic information for the gusset plate being evaluated. Cells that are highlighted in blue represent user input cells while cells highlighted in red represent cells that are inactive. The user begins at the top of the spreadsheet directly under the "*Gusset Plate Inputs & Summary*" cell. Here information such as the user's name, the organization, date and gusset plate ID and the bridge to which the gusset belongs. Additionally there is a drop down tab labeled "*Include Rivets?*". This is here to toggle on or off the rivet evaluation portion of the gusset plate check. At the point when an appropriate rivet strength is chosen for the bridge, the rivet evaluation will be included in the calculated rating factors. Until then, the rivets can be left out. The other tab included in this table is the *Number of Connections* cell. Here the user utilizes the drop down menu to input the number of connections associated with the gusset plate being evaluated. This appropriately highlights the correct number of tables that need to be completed later. The remaining cells that must be filled are the values associated with the condition factor, ϕ_c, and the redundancy factor, ϕ_s. The aforementioned user inputs cells are shown in Figure A-1.

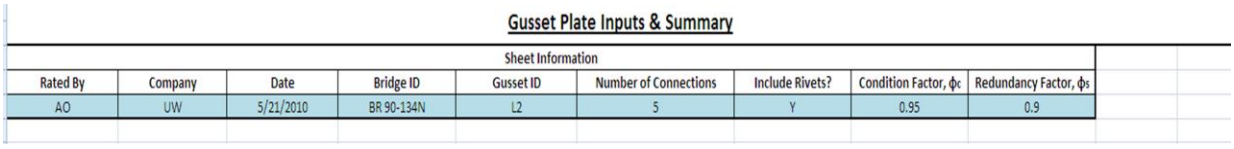

Gusset Plate Inputs & Summary

Sheet Information								
Rated By	Company	Date	Bridge ID	Gusset ID	Number of Connections	Include Rivets?	Condition Factor, ϕc	Redundancy Factor, ϕs
AO	UW	5/21/2010	BR 90-134N	L2	5	Y	0.95	0.9

Figure A-1 First Input Cells in the TEP Spreadsheet.

The next table that needs filled by the user is the *LL Input & RF Summary* table. Here the user inputs the different load cases for which gusset plate connection will be evaluated. For each load case, information such as truck type, live load factors, impact factors and rating methods are inputted directly or selected from a drop down menu. The three cells titled "*Minimum RF*", "*Controlling Connection ID*" and "*Controlling Resistance Type*" will be populated once all of the information for each connection is input in the lower sections of the spreadsheet. These cells provide an executive summary of the controlling RF, the connection that causes this RF as well as the resistance type. A sample of this table can be seen in Figure A-2.

LL Input and RF Summary					Minimum RF	Controlling Connection ID	Controlling Resistance Type
Load Case ID	Live Loads						
	Truck Type	γLL	Impact Factor (I)	Rating Method			
1	HS20 (Inv)	2.17	0.11	LFR			
2	HS20 (Opr)	1.3	0.11	LFR			
3	A1	1.8	0.1	LRFR			
4	A2	1.8	0.1	LRFR			
5	A3	1.8	0.1	LRFR			
6	Legal Lane	1.8	0.1	LRFR			
7	OL1	1.3	0.1	LRFR			
8	OL2	1.3	0.1	LRFR			
9	OL3	1.3	0.1	LRFR			
10	OL4	1.3	0.1	LRFR			
11	OL5	1.3	0.1	LRFR			
12	OL6	1.3	0.1	LFR			

Figure A-2 LL Input and RF Summary Table in the TEP Spreadsheet.

The next table that must be completed by the user is the "*Material & Dimension*" table. Here the user inputs the yield strengths for the gusset plates and splice plates as well as the ultimate strength of the rivets as shown in Figure A-3. The rivet strength cell may be inactive depending on the selection of the "*Include Rivets?*" cell as discussed before. Additionally there are inputs for the number of main gusset plates as well as their thicknesses.

Material & Dimension Inputs							
Gusset Plate Properties		Wind Gusset Plate Properties		Splice Plate Properties		Rivet Properties	
Fy_gp (ksi)	45	Fy_wp (ksi)	45	Fy_sp (ksi)	45	Fu_r (ksi)	40
Thickness, tgp (in)	0.75						
Num Plates, np	2						

Figure A-3 Gusset Plate Property Input in the TEP Spreadsheet.

Triage Procedure Connection Inputs

Connection Information					
Connection ID	Chord or Web?	Splice PL's?	Wind Bracing GP?	Comp. or Tension?	Milled to Bear, Y/N?
L2-L1	Chord	Y	Y	Tension	

Figure A-4 Connection Information Input in the TEP Spreadsheet.

Once the user has input the appropriate values into the preceding tables, evaluation of each connection in the gusset plate begins. This starts by using the "*Connection Information*" table under the "*Triage Procedure Connection Inputs*" section shown in Figure A-4. The first input is the "*Connection ID*" cell. As an example the connection for the member from Joint L1 to Joint L0 is being evaluated. Next the user selects whether the connection corresponds to a chord or web member using the dropdown menu in the "*Chord or Web?*" cell. All diagonals and verticals are considered web members. Next the user uses the drop down menus in the "*Splice PL's?*" and

"*Wind Bracing GP?*" cells to include or exclude the appropriate areas of these supplemental plates for the triage procedure calculation of the chord splices. The next cell, "*Comp. or Tension?*" triggers the inclusion of the buckling check which will be discussed later in these instructions. The final cell in the row is titled "*Milled to Bear?*". This cell can only be triggered when the connection corresponds with a chord that is in compression. If "*Y*" is selected for this cell than the evaluation of the gusset for the chord splice can be stopped because the member is milled to bear and thus the triage approach does not apply since gusset plate buckling is not possible and the rivets provide little to no load transfer. If this is the case, the user can proceed directly to the next connection on the gusset plate (i.e., the connection of a web member to the gusset plate under consideration), otherwise if "N" is selected, than the evaluation proceeds as normal.

The next step in the "*Triage Procedure Connection Inputs*" section is to calculate the yield resistance of the gusset plate connection. This starts by inputting the basic geometry of the connection itself. Parameters such as connection width, w_c, connection length, L_c, and edge length, L_e, are input into their respective cells. It should be noted that the edge length cell will only be active for chord member connections, otherwise this cell will be shaded red.

Next the user inputs the information associated with any splice plates used in the connection. Parameters like splice identification, plate width and thickness are input into the "*Splice ID*", "W_{sp}", and "t_{sp}" cells, respectively. These splice plate input cells will only be activated if the user has input "*Y*" in the "*Splice PL's*" cell, as previously described.

Finally the user inputs parameters associated with any wind bracing gusset plates into the "*Wind Brace GP Dimensions*" table, if this table has been activated by inputting "*Y*" in the "*Wind Bracing GP*" cell. Here information such as brace identification, connection width, connection length, edge distance and wind plate thickness are inputted into the appropriate cells.

Now that all of the pertinent information for the yielding portion of the TEP check have been completed, a resistance, R_n, will be calculated for this connection and is displayed at the end of the section. A sample of the yielding calculation for a gusset plate connection is shown in Figure A-6.

The next section in the connection check is the "*Buckling Resistance Inputs*" section, shown below in Figure A-6. Note that this section is only triggered for members in compression that are not milled to bear. Here the only main user input is the centroidal buckling length in the

"*Centroidal Length, L_cnt*" cell. If the user so desires, the recommended values for the compression resistance factor, ϕ_c, and the effective length factor, *K*, can be changed as well, but the use of the default values is recommended. The rest of the cells show the values needed calculate the buckling resistance value, R_n. A sample calculation for buckling resistance is shown in Figure A-6.

.

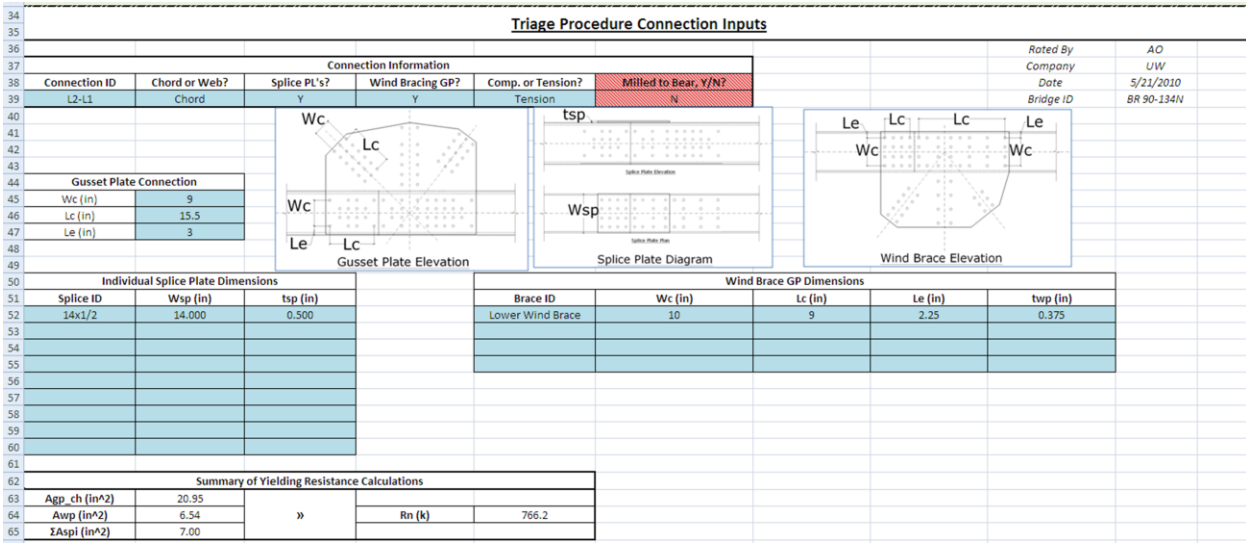

Figure A-5 TEP Yield Check in the TEP Spreadsheet.

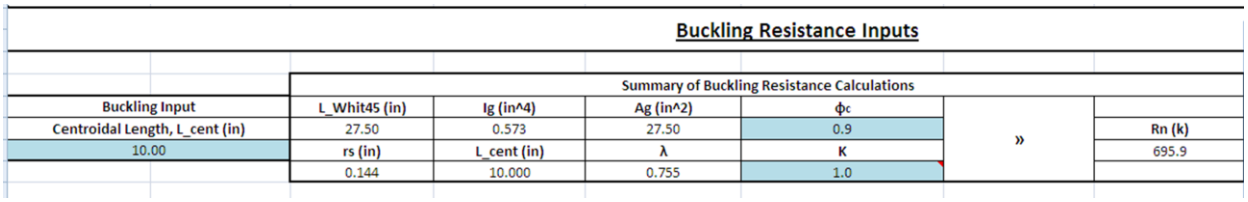

Figure A-6 Buckling Check in the TEP Spreadsheet.

The next section in the connection evaluation is the "*Rivet Resistance Inputs*" section shown below. This section is only triggered when the user selects "*Y*" in the "*Include Rivets?*" cell, as discussed previously, otherwise it remains inactive. Here the user inputs the diameter of the rivets into the "*Rivet Diameter,D_r*" cell as well as the number single shear and double shear rivets into the "*# of Single Shear Rivets, nss*" and "*# of Double Shear Rivets, nds*" cells respectively. Using these inputs, the rivet resistance, Pr, is calculated as shown in Figure A-7.

Rivet Input			»	Rivet Resistance
Rivet Diameter, D_r (in)	# of Single Shear Rivets, nss	# of Double Shear Rivets, nds		Pr (k)
0.9	45	30		2671.9

Figure A-7 Rivet Check in the TEP Spreadsheet.

Now that all of the pertinent resistances for the connection in question have been calculated, the user then moves on to the "*Rating Factors*" section of the spreadsheet. At the top of this section there are two cells, shown in Figure A-7, that show the controlling resistance in kips as well as the corresponding type of resistance. Note that is the connection is milled to bear, than these cells will be highlighted yellow and "*Milled to Bear*" will be written inside.

Controlling Resistance (k)	Resistance Type
1623.7	Buckling

Figure A-8 Controlling Resistance in the TEP Spreadsheet.

Next, the user inputs the appropriate values for the dead load factors and loads for LFR and LRFR rating methods. An example of these tables is shown in Figure A-9.

Dead Load Factoring			
Rating Method	LFR	»	Factored DL (k)
γDL	1.2		1200
Dead Load (k)	1000		
Rating Method	LRFR	»	Factored DL (k)
γDL_C	1.2		135
DL_C (k)	50		
γDL_W	1.5		
DL_W (k)	50		

Figure A-9 Dead and Live Load Factor Inputs in the TEP Spreadsheet.

Next the user moves onto the "*LL Input and RF Summary*" portion of the table. Here all of the information entered in the *"LL Input & RF Summary*" table has been migrated down and is shown merely as a reminder of all the load cases for which the connection will be evaluated. The only user input in this table is the live load that the connection experiences for each load case. This live load, as well as the previously inputted dead loads, is used to calculate RF's for each resistance type for the connection in question. The resistance type that produces the lowest RF's

is the controlling resistance and the RF's it produces are highlighted. A sample of this table is shown in Figure A-10.

Rating Factors

Controlling Resistance (k)	Resistance Type
695.9	Buckling

Dead Load Rating Method			
Rating Method	LFR	»	Factored DL (k)
γDL	1.2		294.6
Dead Load (k)	245.5		

Rating Method	LRFR	»	Factored DL (k)
γDL_C	1.2		304.02
DL_C (k)	214.6		
γDL_W	1.5		
DL_W (k)	31		

Controlling RF	

LL Input and Connection RF Summary						Resistance Type		
	Live Loads					Yielding	Buckling	Rivets
Load Case ID	Truck Type	γLL	Impact Factor (I)	Rating Method	Member LL (k)	RF	RF	RF
1	HS20 (Inv)	2.17	0.11	LFR	99.4	2.51	2.17	3.49
2	HS20 (Opr)	1.3	0.11	LFR	99.4	4.19	3.62	5.83
3	A1	1.8	0.1	LRFR	110	2.12	1.80	3.04
4	A2	1.8	0.1	LRFR	115	2.03	1.72	2.91
5	A3	1.8	0.1	LRFR	120	1.95	1.65	2.79
6	Legal Lane	1.8	0.1	LRFR	125	1.87	1.58	2.68
7	OL1	1.3	0.1	LRFR	140	2.31	1.96	3.31
8	OL2	1.3	0.1	LRFR	155	2.09	1.77	2.99
9	OL3	1.3	0.1	LRFR	170	1.90	1.61	2.73
10	OL4	1.3	0.1	LRFR	195	1.66	1.41	2.38
11	OL5	1.3	0.1	LRFR	225	1.44	1.22	2.06
12	OL6	1.3	0.1	LFR	250	1.68	1.45	2.34

Figure A-10 Rating Factor Summary Table in the TEP Spreadsheet.

When the user completes the *Rating Factor* section than evaluation of this particular connection is complete and the process repeats itself for each connection in the gusset plate. Once this is complete the user then scrolls to the very top of the spreadsheet to find that the remainder of the "*LL Input & RF Summary*" table has been populated and that the executive summary of this particular gusset plate is complete. When the user prints the spreadsheet, the executive summary is printed separately followed by a separate page for each individual connection. A sample of the executive summary is shown in Figure A-11.

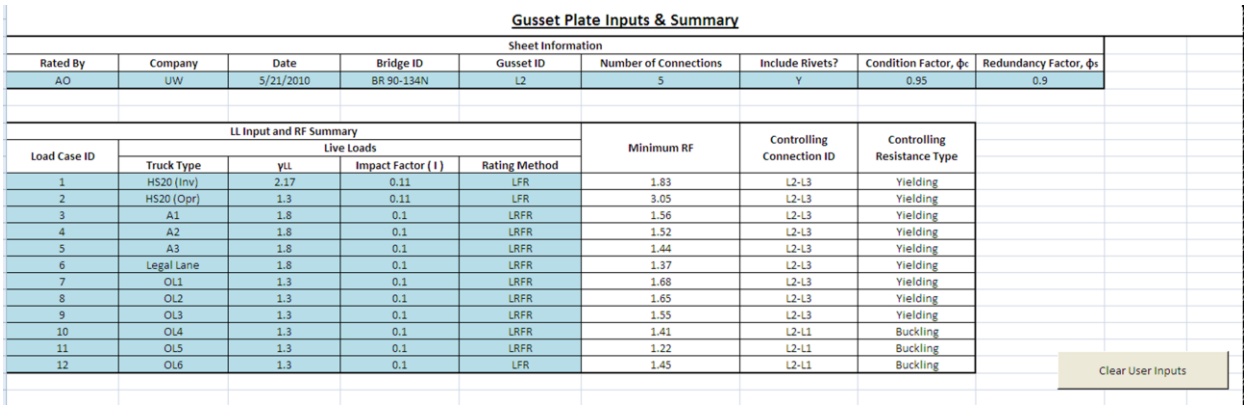

Gusset Plate Inputs & Summary

Sheet Information								
Rated By	Company	Date	Bridge ID	Gusset ID	Number of Connections	Include Rivets?	Condition Factor, ϕ_c	Redundancy Factor, ϕ_s
AO	UW	5/21/2010	BR 90-134N	L2	5	Y	0.95	0.9

LL Input and RF Summary							
Load Case ID	Live Loads				Minimum RF	Controlling Connection ID	Controlling Resistance Type
	Truck Type	γ_{LL}	Impact Factor (I)	Rating Method			
1	HS20 (Inv)	2.17	0.11	LFR	1.83	L2-L3	Yielding
2	HS20 (Opr)	1.3	0.11	LFR	3.05	L2-L3	Yielding
3	A1	1.8	0.1	LRFR	1.56	L2-L3	Yielding
4	A2	1.8	0.1	LRFR	1.52	L2-L3	Yielding
5	A3	1.8	0.1	LRFR	1.44	L2-L3	Yielding
6	Legal Lane	1.8	0.1	LRFR	1.37	L2-L3	Yielding
7	OL1	1.3	0.1	LRFR	1.68	L2-L3	Yielding
8	OL2	1.3	0.1	LRFR	1.65	L2-L3	Yielding
9	OL3	1.3	0.1	LRFR	1.55	L2-L3	Yielding
10	OL4	1.3	0.1	LRFR	1.41	L2-L1	Buckling
11	OL5	1.3	0.1	LRFR	1.22	L2-L1	Buckling
12	OL6	1.3	0.1	LFR	1.45	L2-L1	Buckling

Clear User Inputs

Figure A-11 Executive Summary Table in the TEP Spreadsheet.